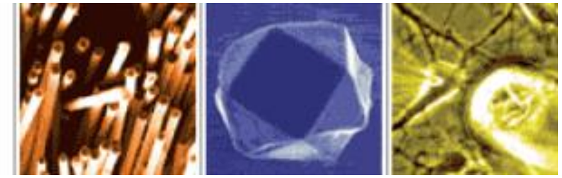

Watching nanomaterials with X-ray eyes: from nanoparticles to real devices

Lorenzo Mino

Department of Chemistry and NIS, University of Torino

School on Synchrotron Radiation “Gilberto Vlaic”, 16-26 September 2024

Nanomaterials

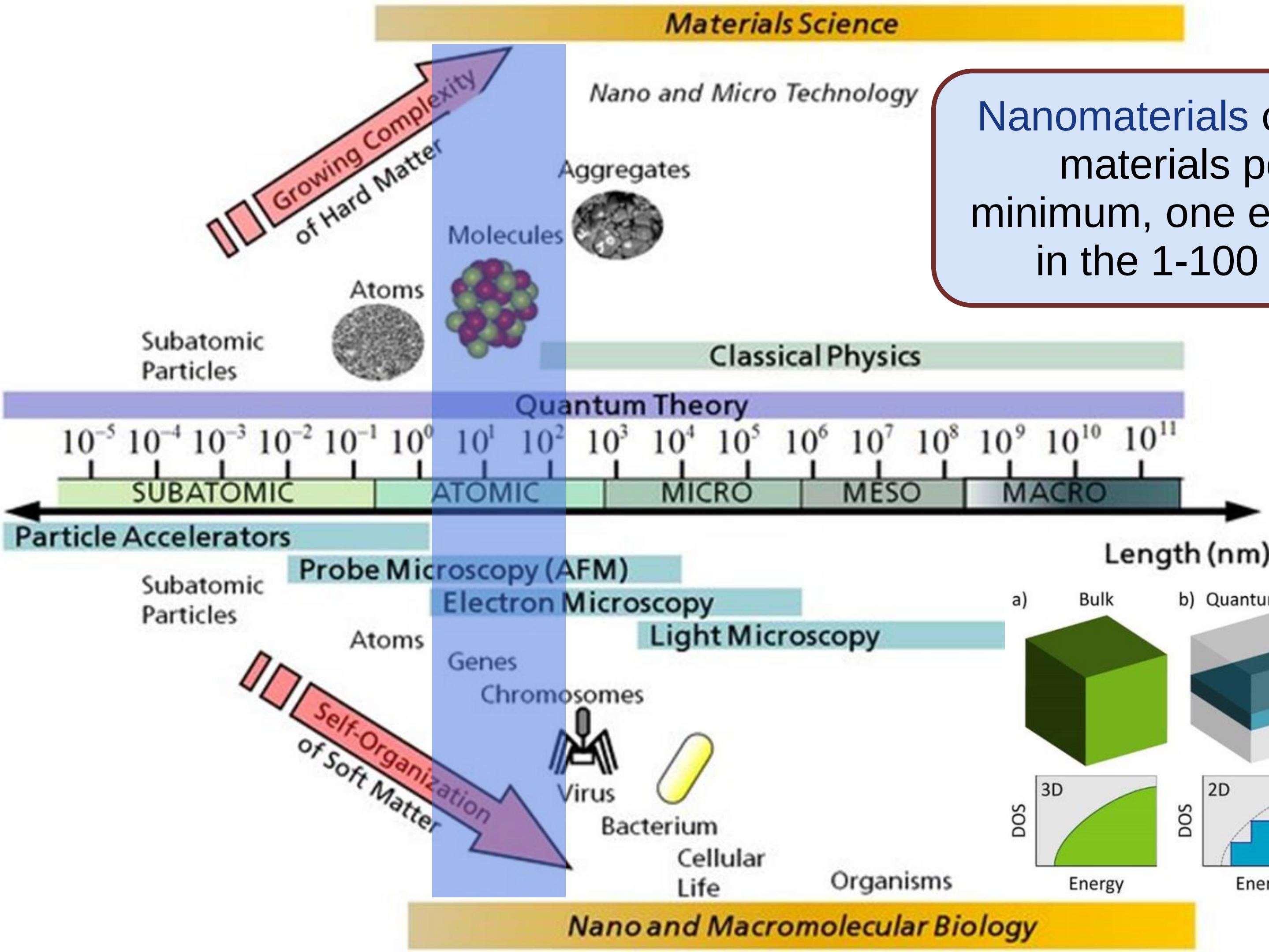

Nanomaterials can be defined as materials possessing, at minimum, one external dimension in the 1-100 nm size range

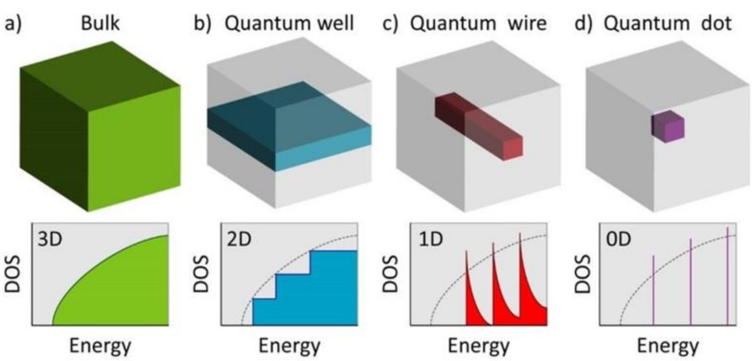

Nanotechnology: unintentional beginning

Lycurgus Cup

4th-century, its red color derives from enclosed Au particles in the size range 5–60 nm. Classical Mie scattering changes the colur of transmitted light

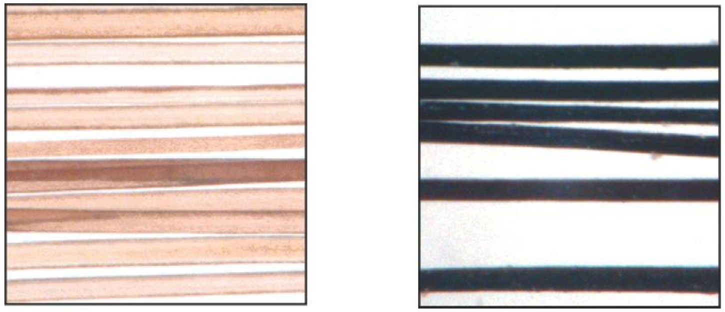

Ancient Hair Dyeing Formula

Hair-blackening recipe originating from the Greco-Roman period, based on a mixture of PbO and $Ca(OH)_2$ with a small amount of water, has been shown to work by the formation of 5-nm PbS nanocrystals inside the hair cortex

Nanotechnology: unintentional beginning

Gold and silver nanoparticles can be used to produce stained glass windows.

Silver - spheres
Size: 40 nm
Reflected color: Dark blue
1

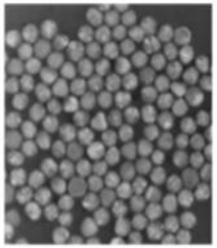

Silver - spheres
Size: 80 nm
Reflected color: Celestial blue
2

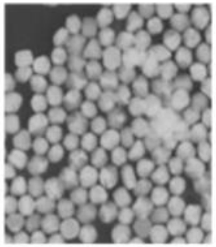

Silver - spheres
Size: 100 nm
Reflected color: Shiny gold
3

Medieval stained glass

Schott glasses

Optical filters with different cut-off frequencies

Nanotechnology: conceptual origins

There's Plenty of Room at the Bottom

29 December 1959, annual meeting of the American Physical Society, California Institute of Technology (Caltech)

Richard Feynman
(Nobel Prize in Physics 1965)

Norio Taniguchi
Coined the term «nano-technology» in 1974 referring to «ultra precision materials processing technologies»

Nanomaterials applications

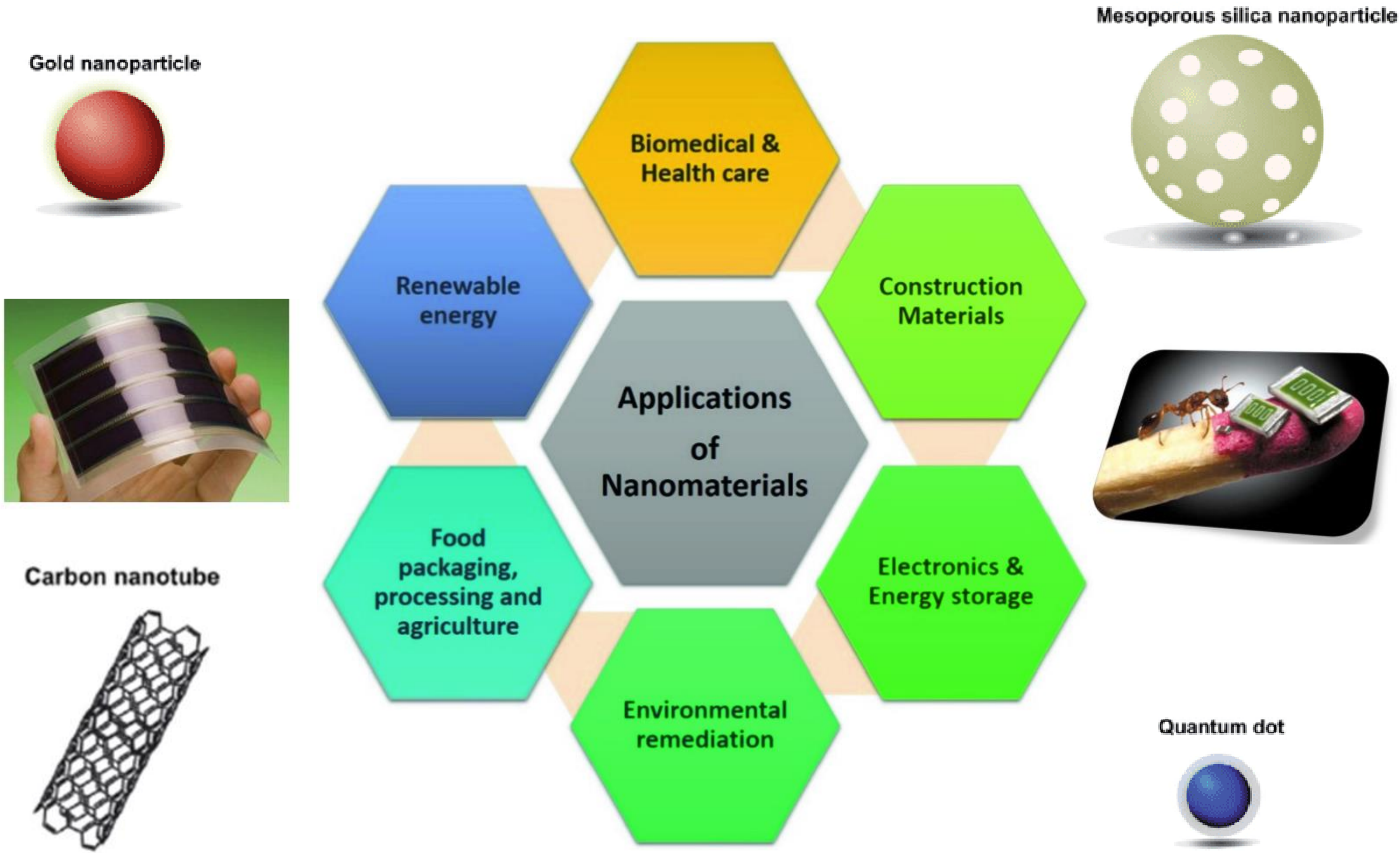

Nanomaterials market

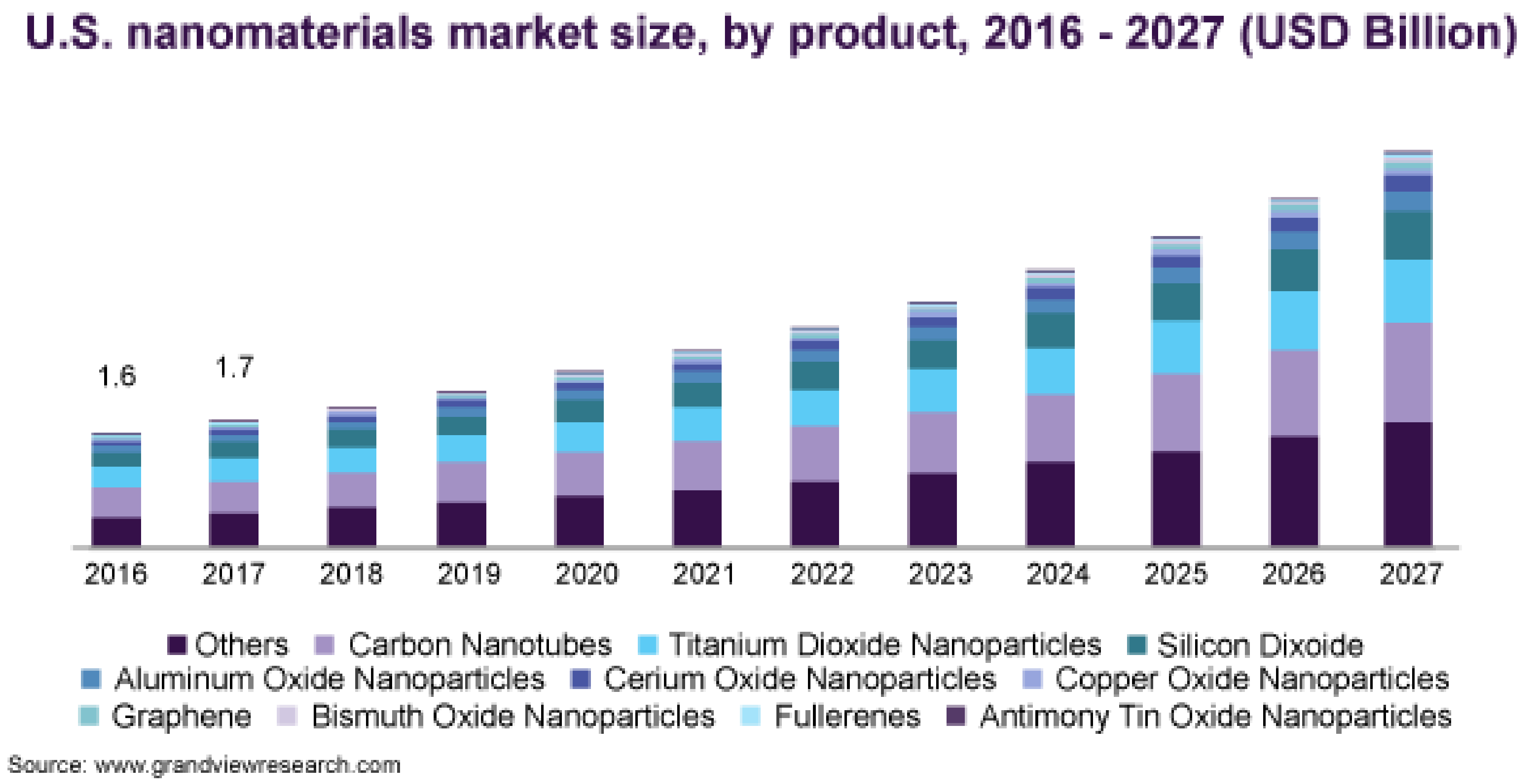

Nanomaterials properties

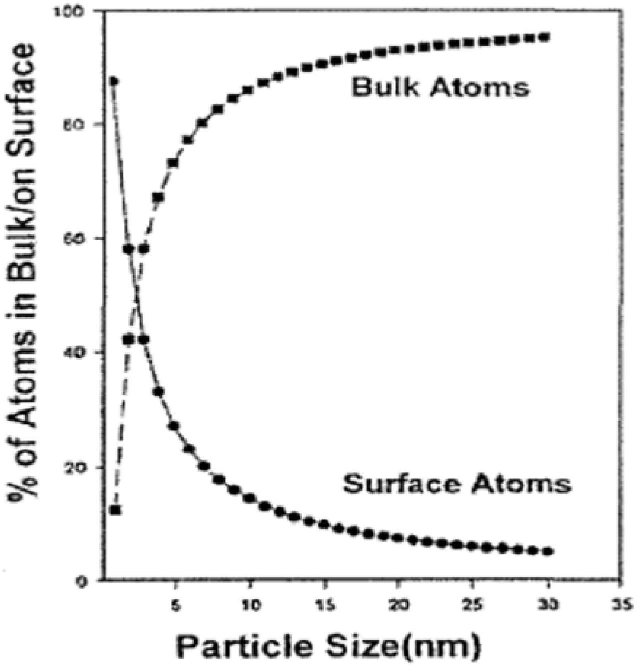

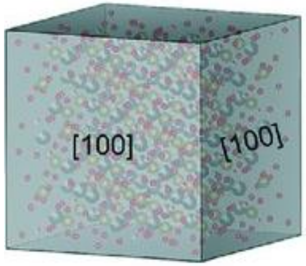

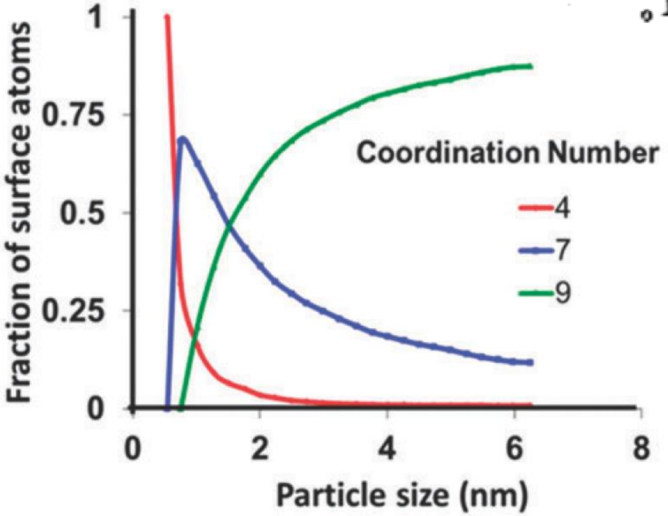

Catalytic activty is strongly shape and size dependent

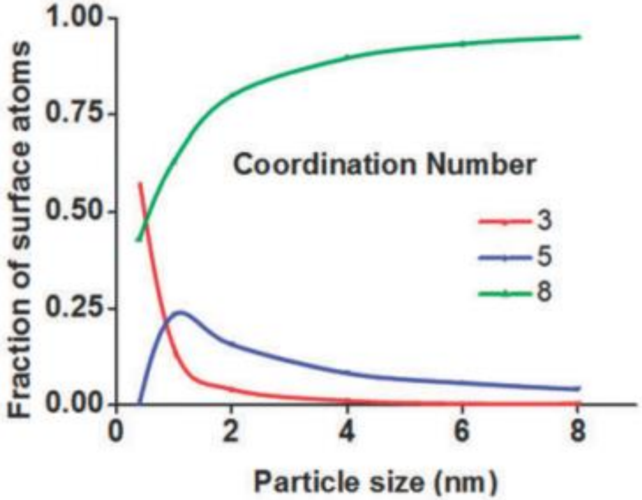

S.Cao et al., Chem. Soc. Rev., 2016, 45, 4747--4765

Nanomaterials properties

Au NPs optical properties

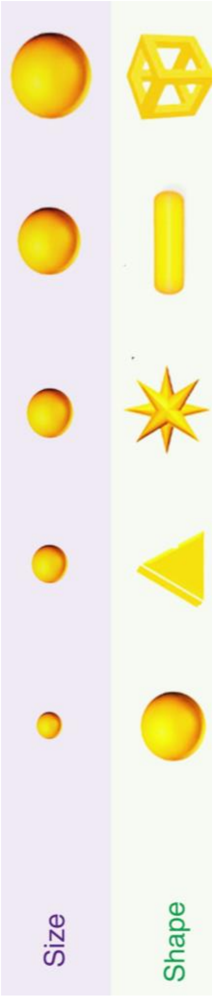

Size **Shape** **Interparticle distance**

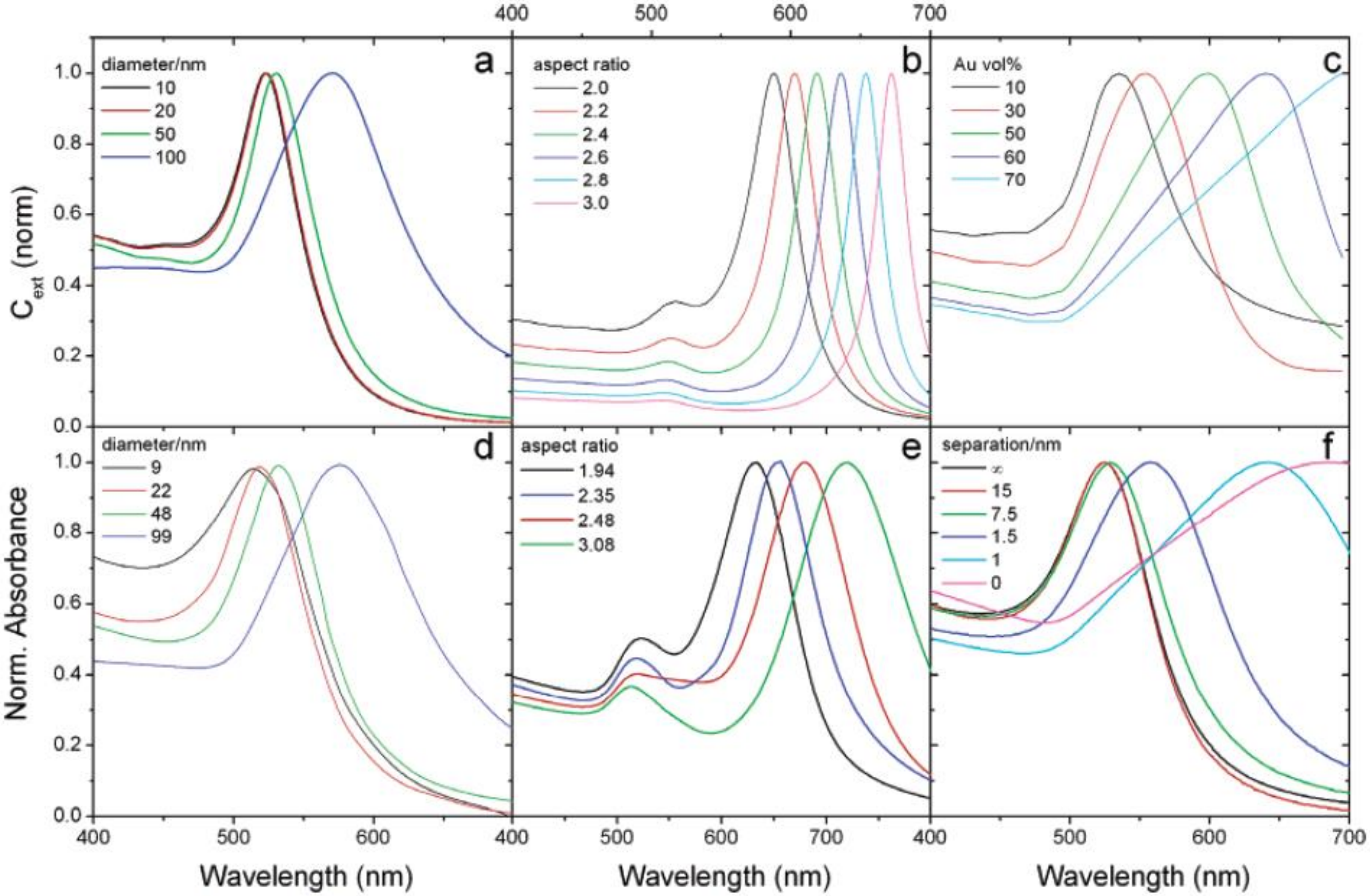

Top: Calculated UV−visible spectra for (a) Au spheres with varying diameters, (b) Au ellipsoids of varying aspect ratio, and (c) thin glass films loaded with increasing Au nanoparticle volume fractions. Bottom: Experimental spectra for (d) Au spheres,[40] (e) Au nanorods, and (f) multilayer films of glass-coated Au spheres with varying interparticle distance.

Probing different lenght scales

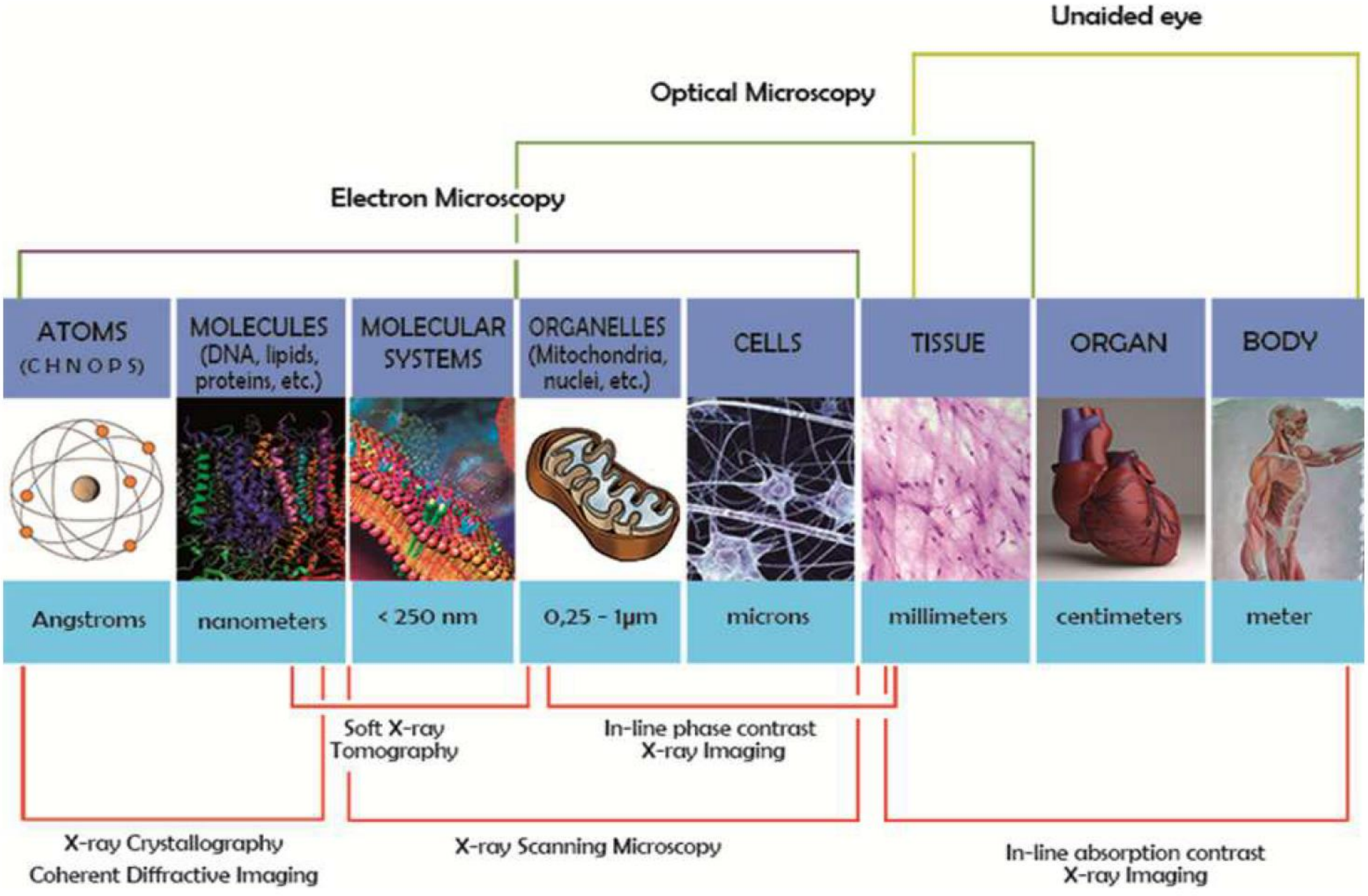

Let's start with a simple case: nanoparticles…

TiO_2 as model system

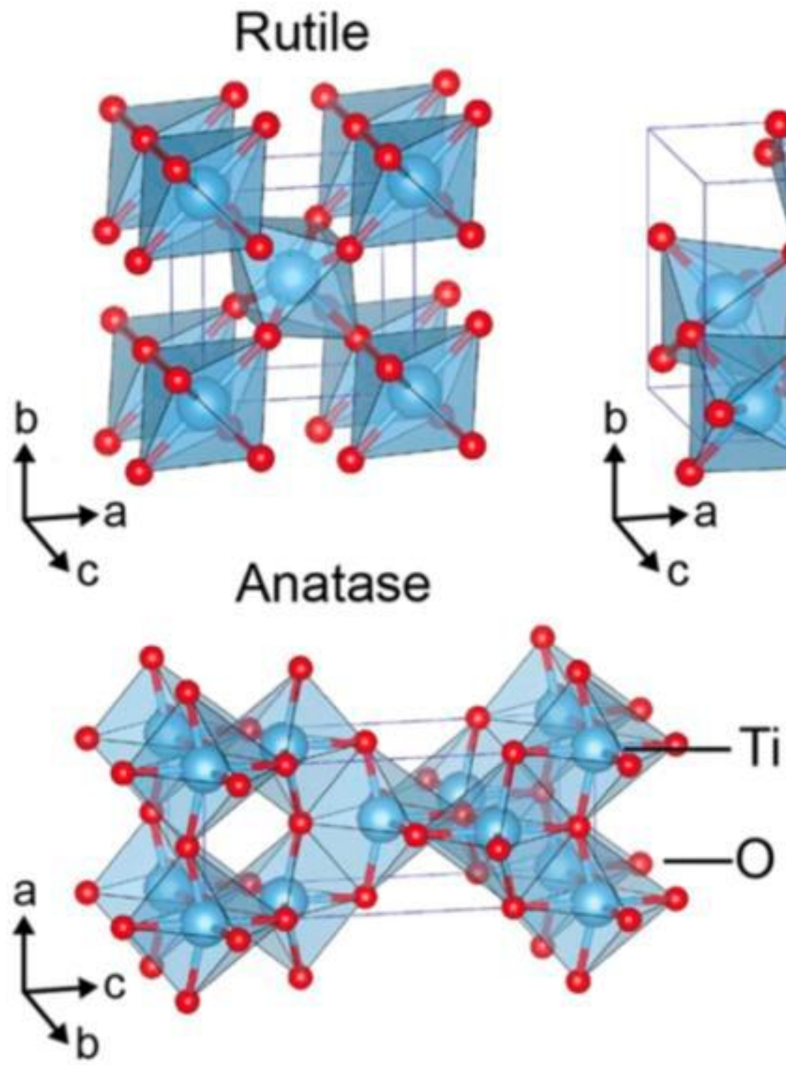

TiO_2 applications

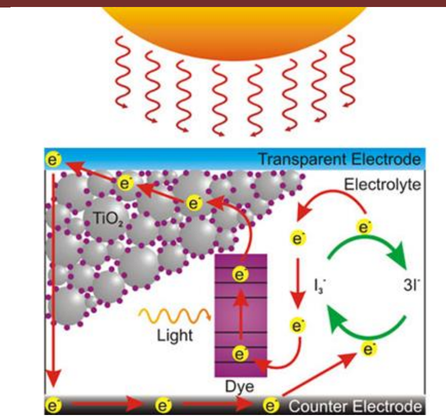

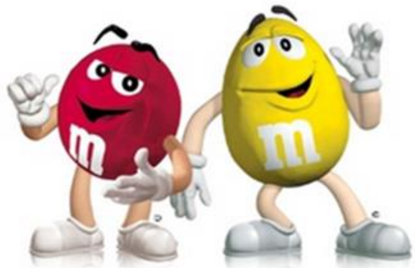

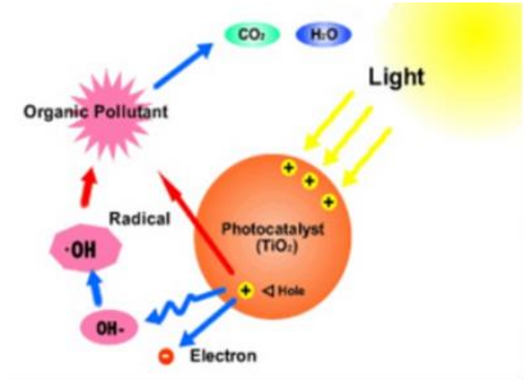

TiO_2 photocatalysis

Photocatalysis

Acceleration of a chemical reaction induced by photoabsorption by a solid material (the "photocatalyst"), which remains unchanged during the reaction

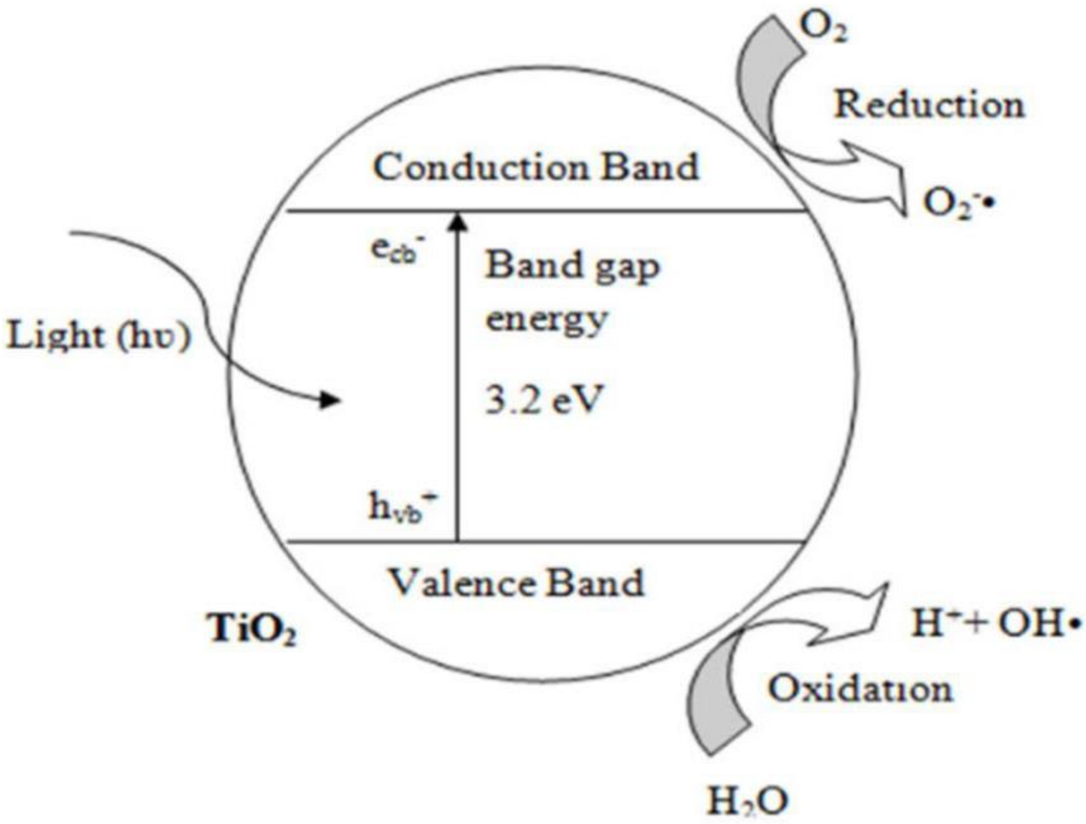

$$hv + TiO_2 \rightarrow e^- + h^+$$

electron-hole pairs formation

$$A(ads) + e^- \rightarrow A^-(ads)$$

reduction of adsorbed species

$$D(ads) + h^+ \rightarrow D^+(ads)$$

oxidation of adsorbed species

e^--h^+ lifetime is crucial (defects, crystallinity…)

Importance of TiO_2 NP size

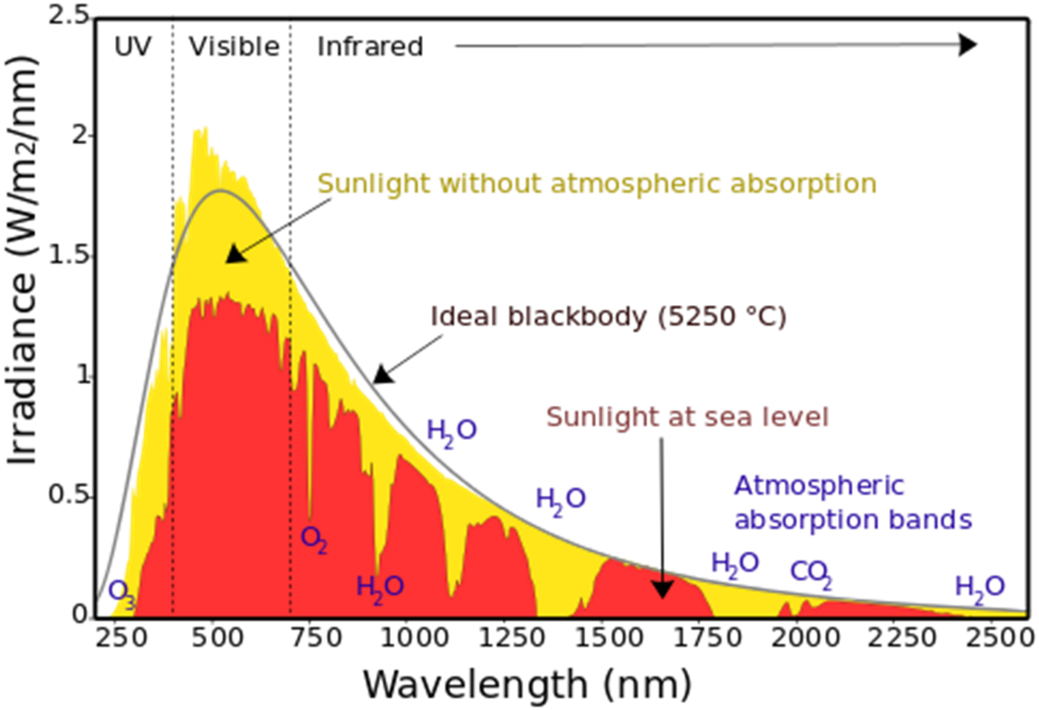

Spectrum of solar radiation

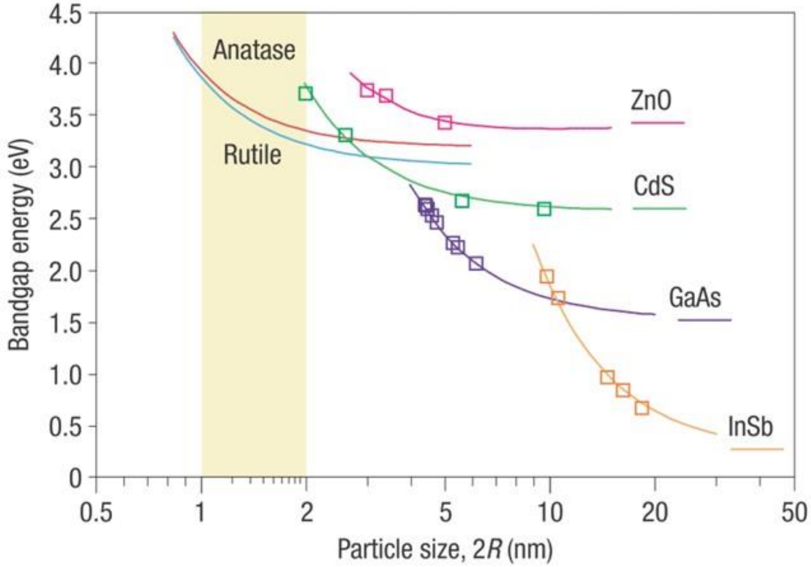

Quantum size effect

N. Satoh et al., Nature Nanotech 2008, 3, 106–111

Importance of TiO_2 NP shape

Facet-dependent band gap

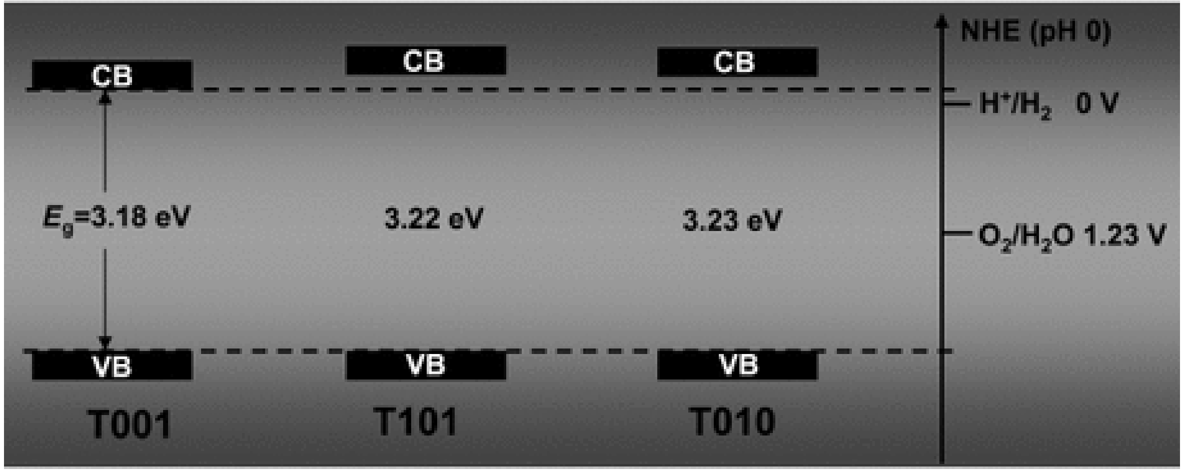

J. Pan et al., Angew. Chem. Int. Ed. 2011, 50, 2133 –2137

Facet-dependent charge carriers migration

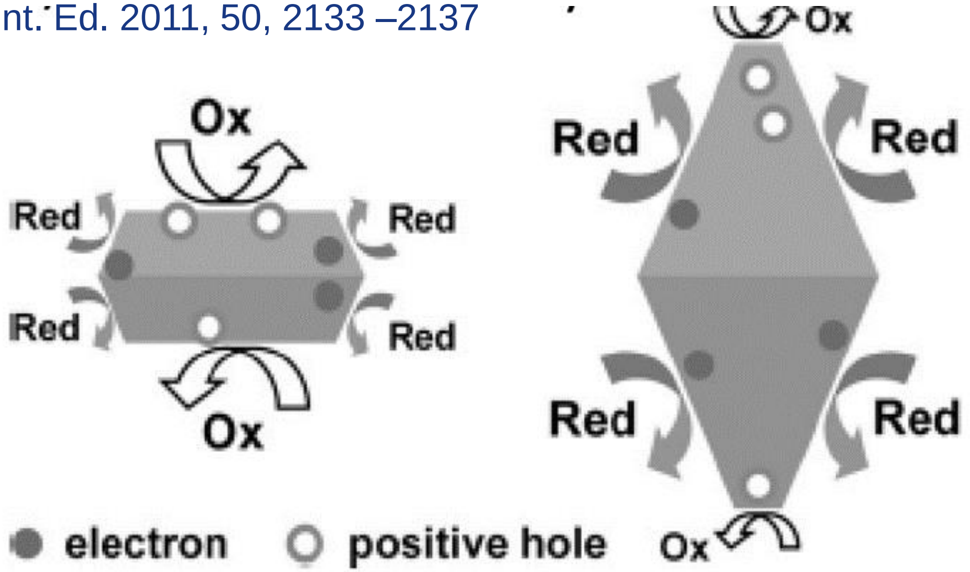

X-ray techniques in nanoparticles characterization

Shape and size engineered TiO_2 nanoparticles0

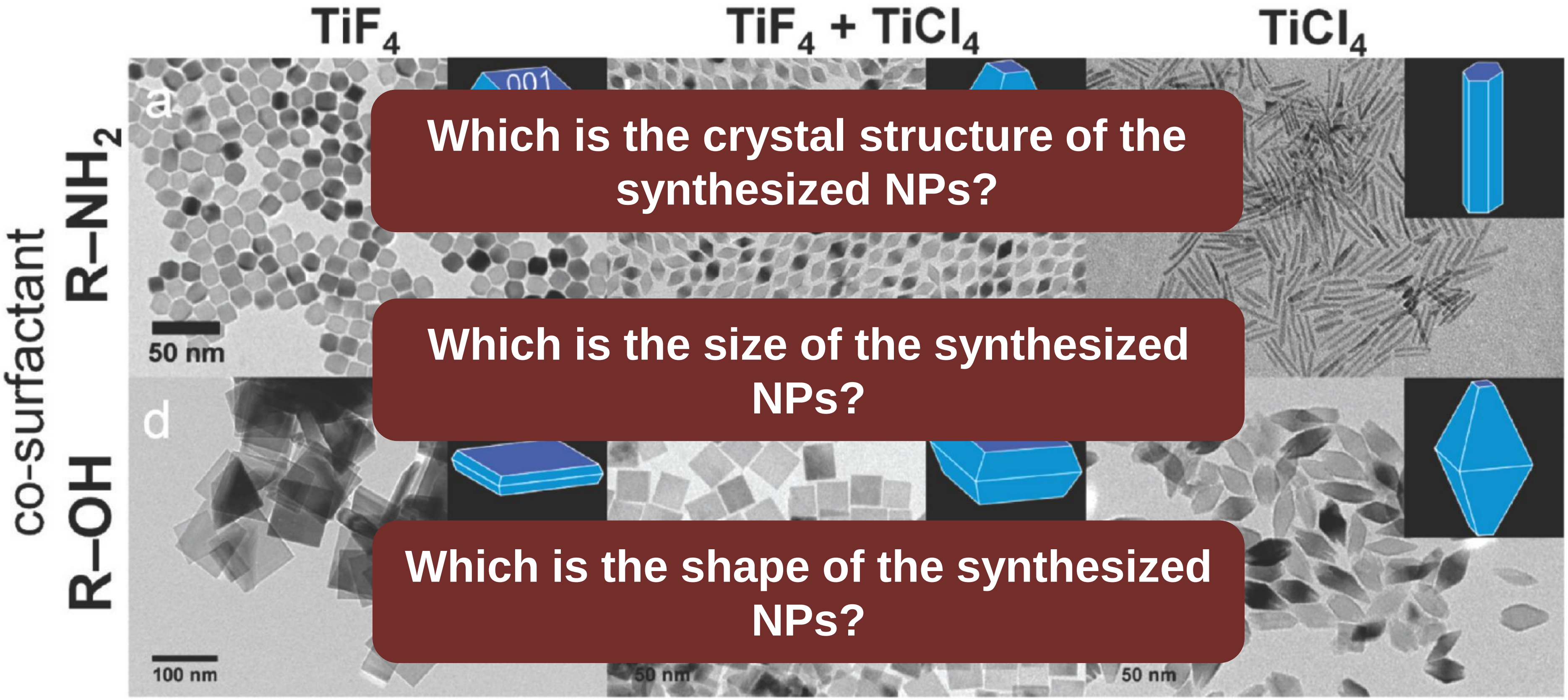

Which is the crystal structure of the synthesized NPs?

Which is the size of the synthesized NPs?

Which is the shape of the synthesized NPs?

T.. Gordon et al., J. Am. Chem. Soc. 2012, 134, 6751 − 6761

Which is the NPs crystal structure?

Bragg law: $$d = \frac{\lambda}{2\sin\theta} = \frac{2\pi}{\left[\frac{4\pi}{\lambda}\right]\sin\theta} = \frac{2\pi}{q}$$

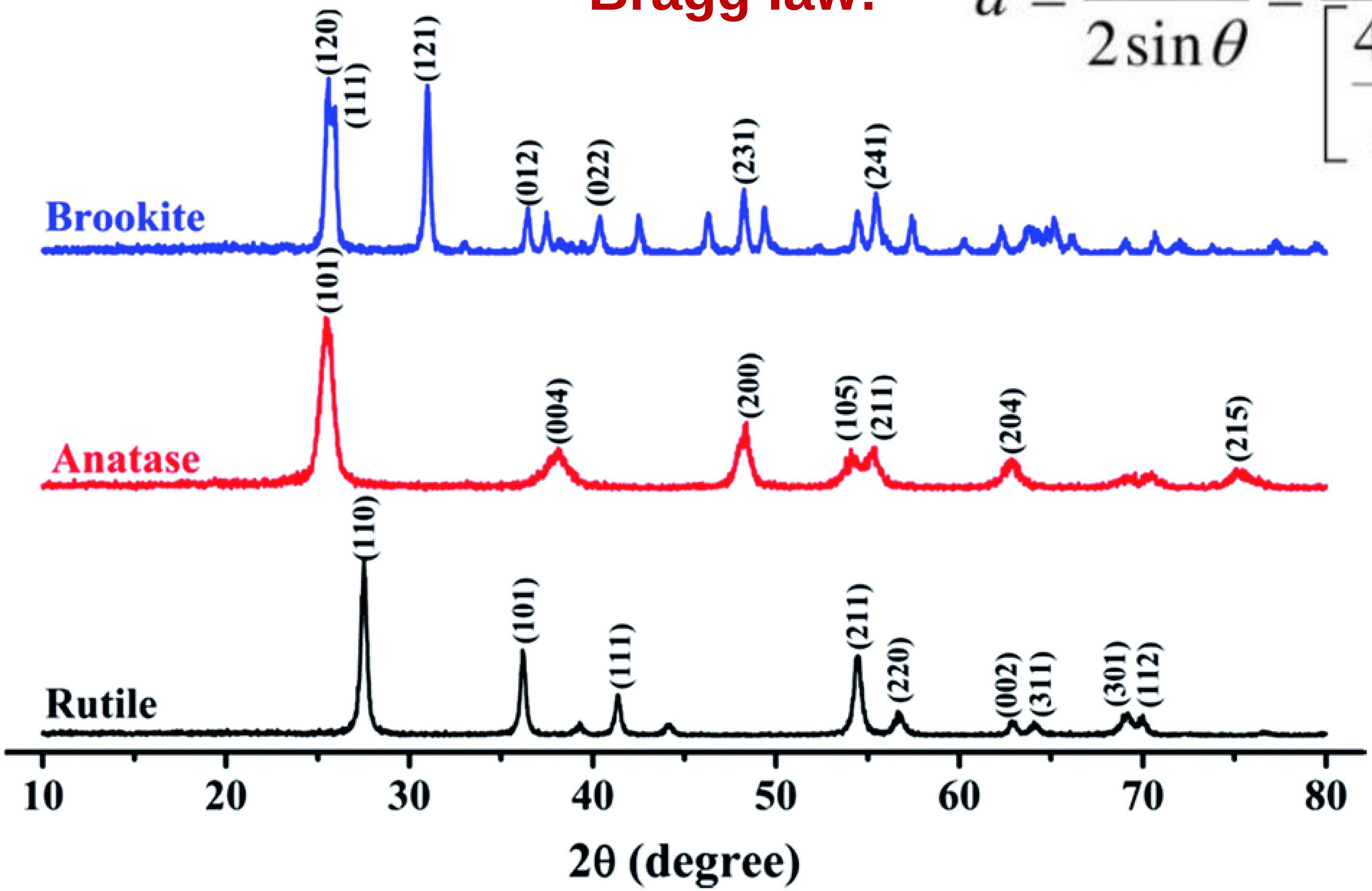

Which is the NPs crystal structure?

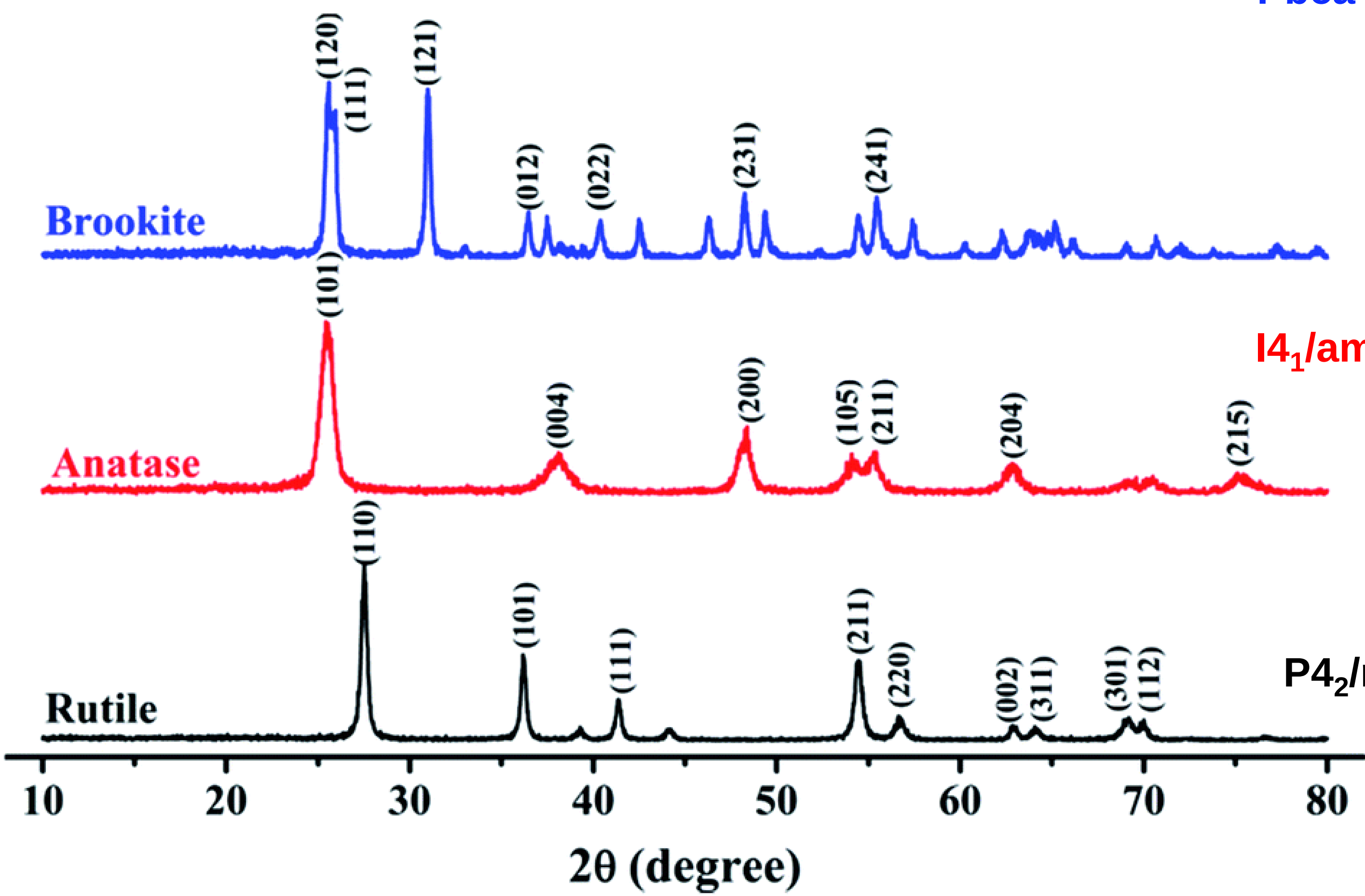

Pbca

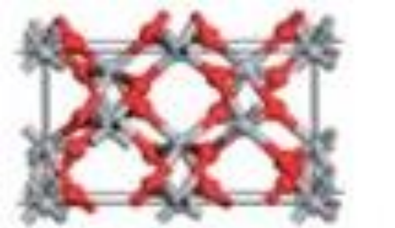

a = 5.455 Å
b = 9.181 Å
c = 5.142 Å

$I4_1/amd$

a = b = 3.785 Å
c = 9.512 Å

$P4_2/mnm$

a = b = 4.593 Å
c = 2.959 Å

Which is the NPs size?

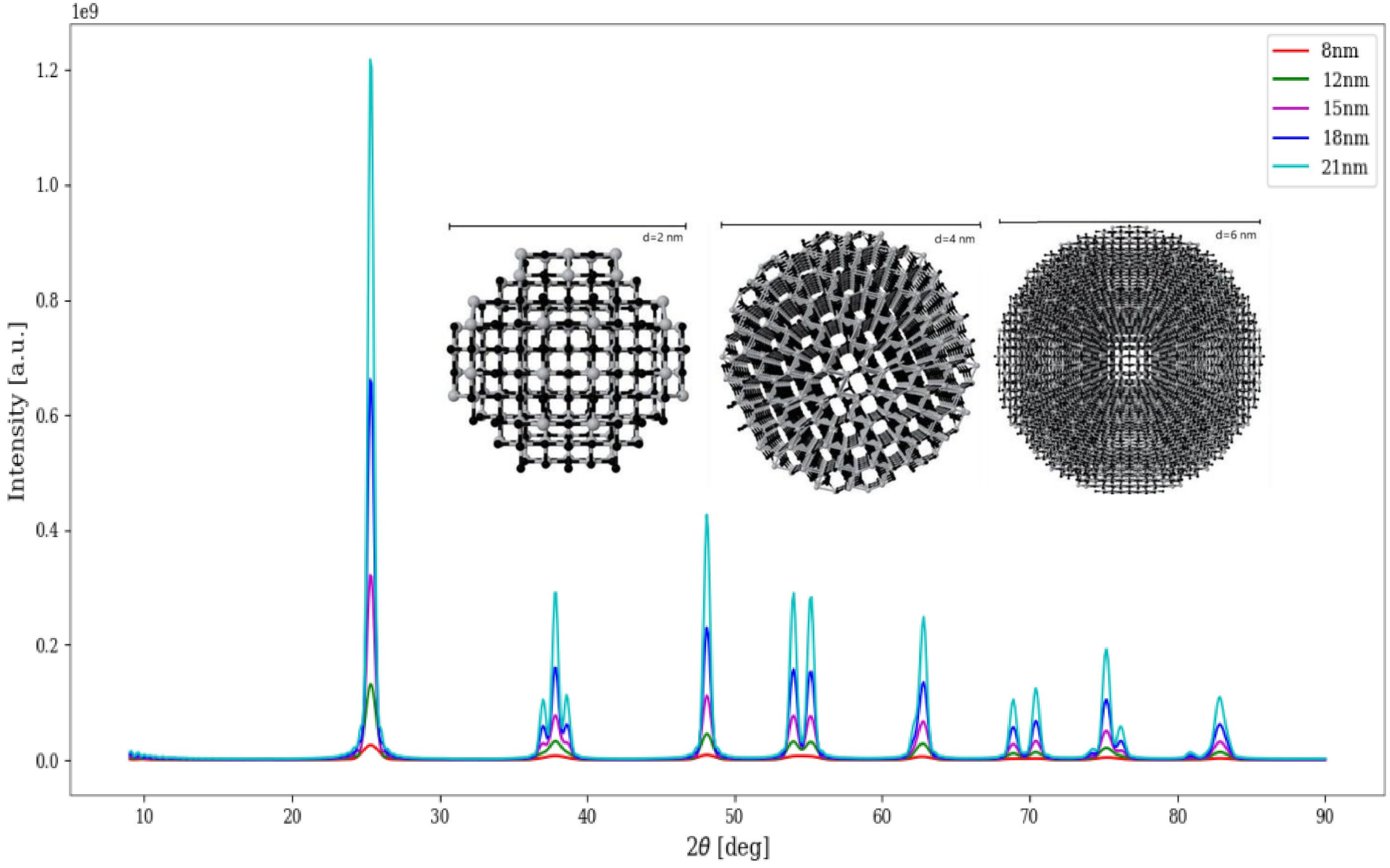

Scherrer equation:

$$L = \frac{K\lambda}{(\beta_{exp} - \beta_{strum})\cos\theta}$$

Monitoring NP sintering and phase transitions

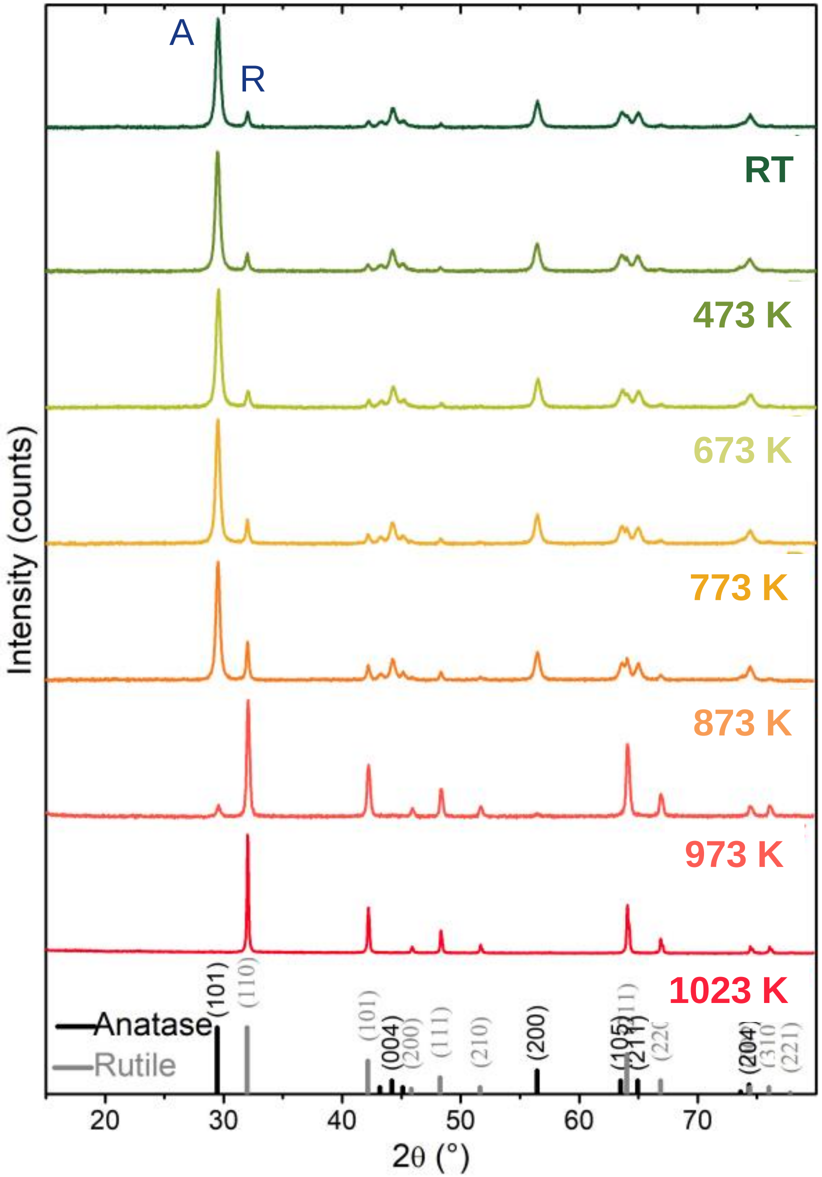

Temperature of treatments[a]	Phase composition[b]		Crystallite sizes[c]	
	Anatase (wt%)	Rutile (wt%)	Anatase (nm)	Rutile (nm)
RT	83	17	28	47
473 K	83	17	28	47
673 K	83	17	28	47
773 K	80	20	33	56
873 K	59	41	35	60
973 K	7	93	48	62
1,023 K		100		237

M. J. Uddin et al., Front. Mater. 2020, 7, 192.

Which is the NPs shape?

J. Liu et al., Chem. Mater. 2017, 29, 5591−5604

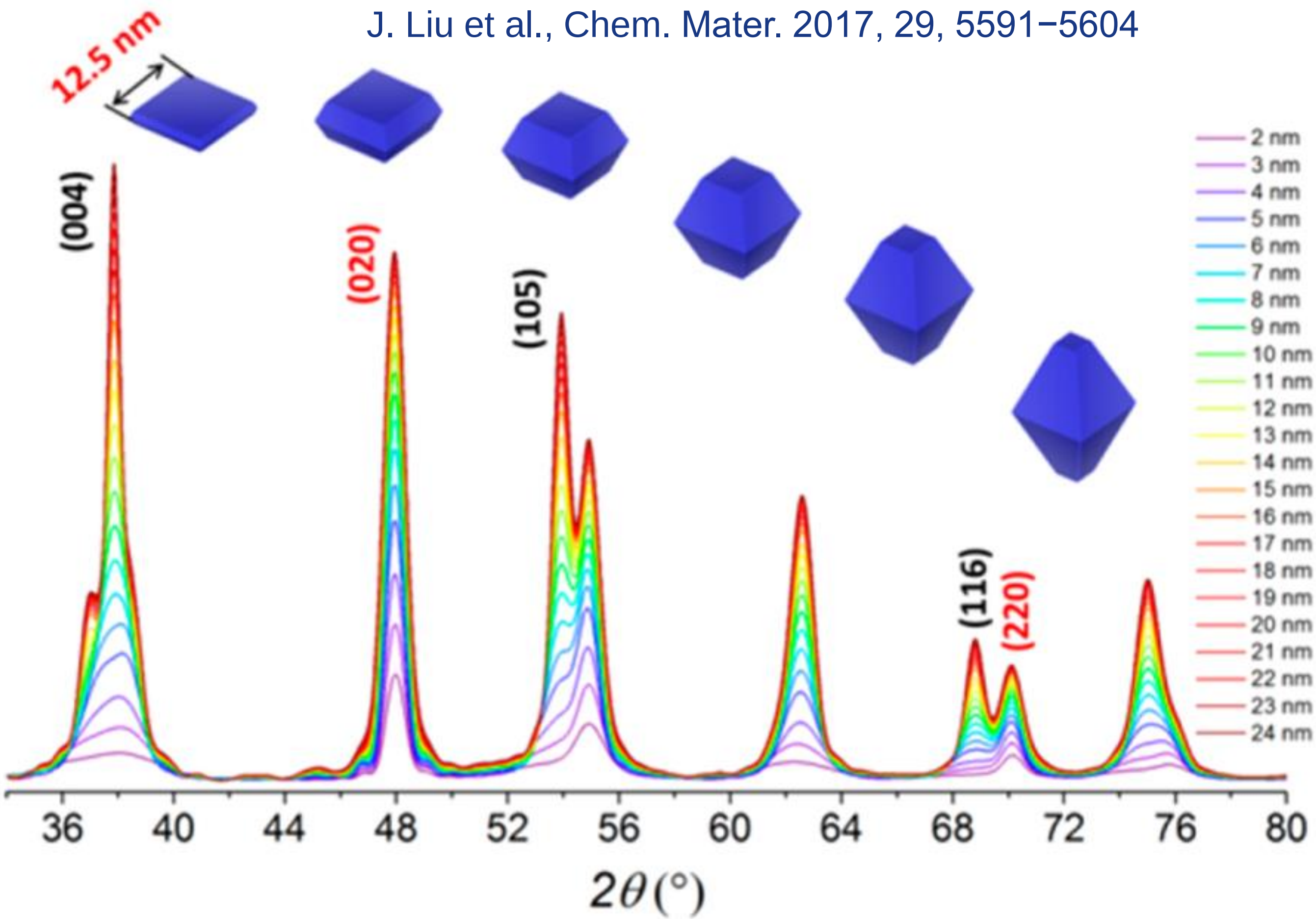

The relative intensity and FWHM of the XRD peaks depends on the NPs shape

Small angle X-ray scattering (SAXS)

Technique	d (nm)	q (nm^{-1})	q ($Å^{-1}$)	θ(deg) for λ=1.5405Å
SAXS/SAXD	100	0.063	0.0063	0.044
SAXS/SAXD	10	0.63	0.063	0.44
WAXS/WAXD	1	6.3	0.63	4.4
WAXS/WAXD	0.1	63	6.3	50.6

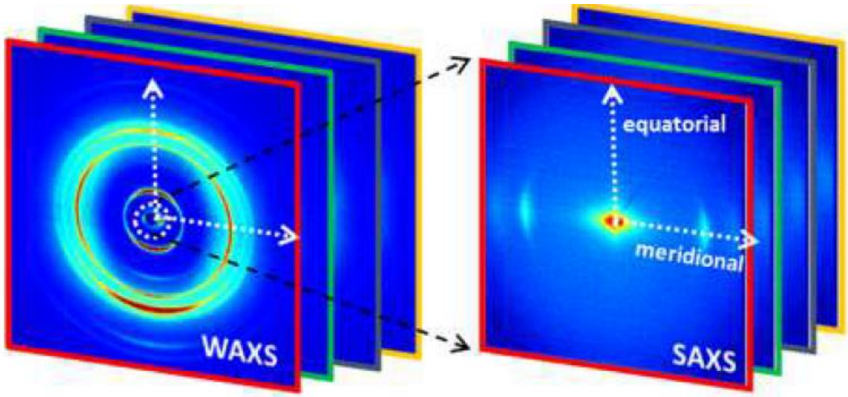

$$d = \frac{\lambda}{2\sin\theta} = \frac{2\pi}{\left[\frac{4\pi}{\lambda}\right]\sin\theta} = \frac{2\pi}{q}$$

C. Giannini et al., Prog. Mater. Sci. 2020, 112, 100667

SAXS: shape and size

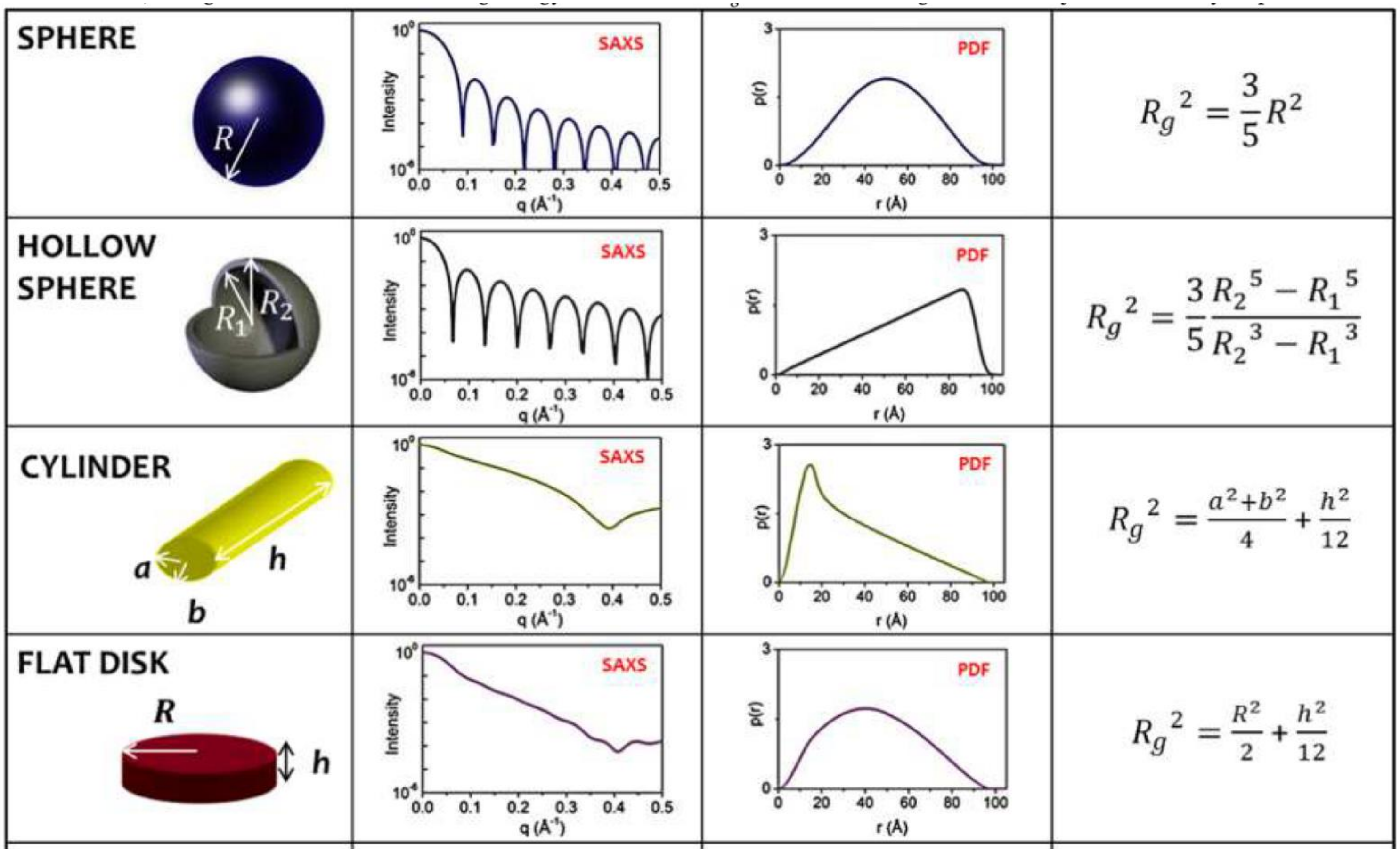

The gyration radius (R_g) can be linked to the main dimensions of the object

C. Giannini et al., Prog. Mater. Sci. 2020, 112, 100667

The Debye scattering equation

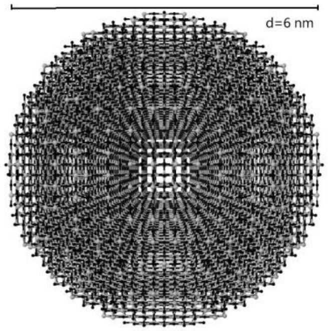

$$I(q) = I_0 \sum_m \sum_n F_m F_n \frac{\sin(qr_{mn})}{qr_{mn}}$$

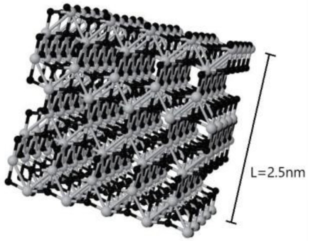

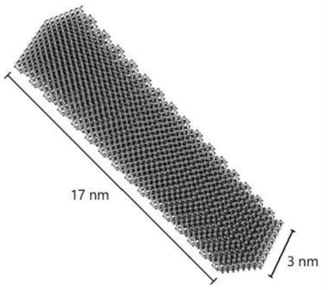

r_{mn} is the distance between atoms m and n, with atomic form factors F_m and F_n,

The Debye approach holds for both small and wide angle scattering data, and it is applicable to crystalline, partially crystalline and amorphous samples.

Combining SAXS and WAXS

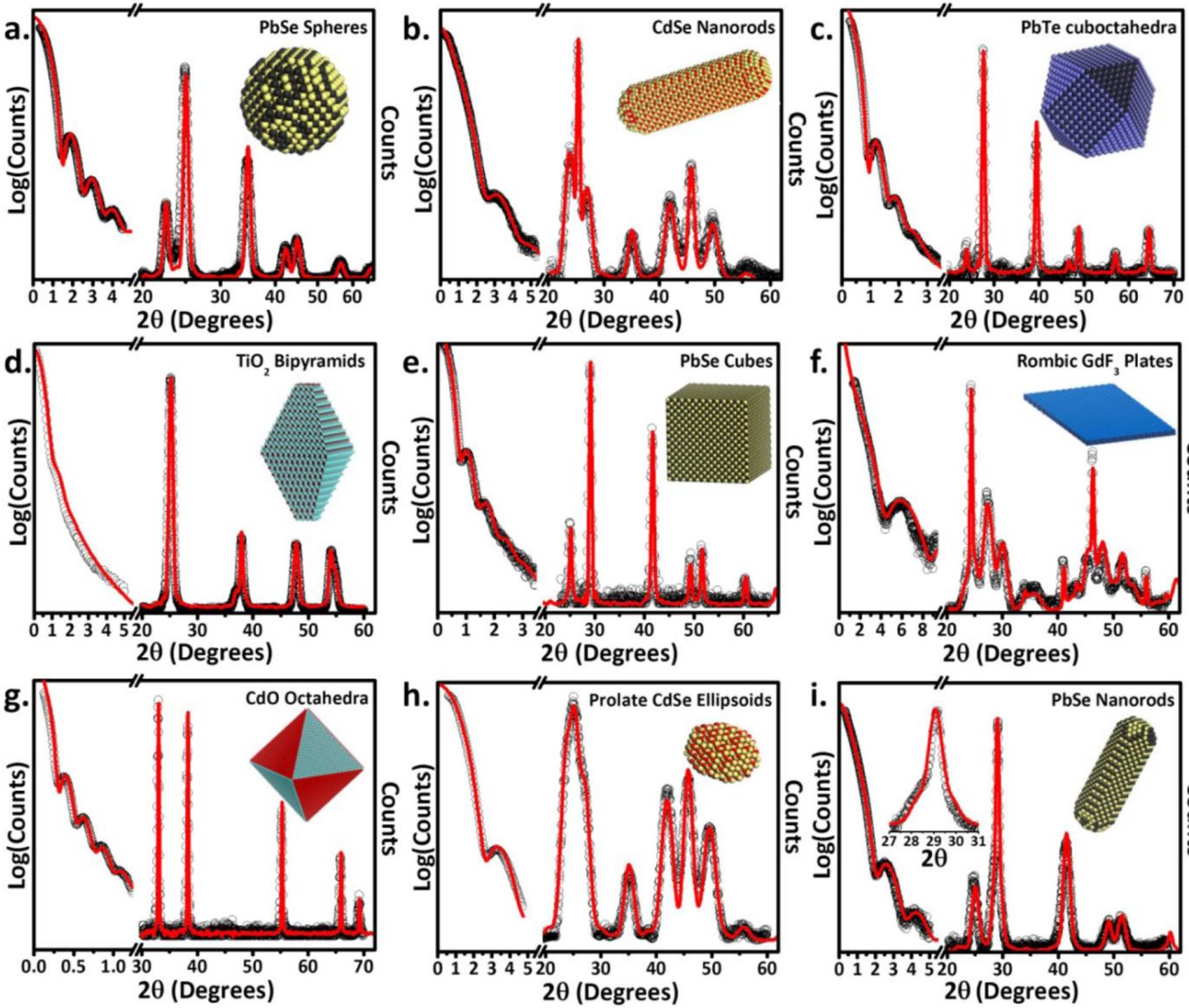

T. Gordon et al., Chem. Mater. 2015, 27, 2502−2506

Why X-rays and not electron microscopy?

Shape-controlled NPs

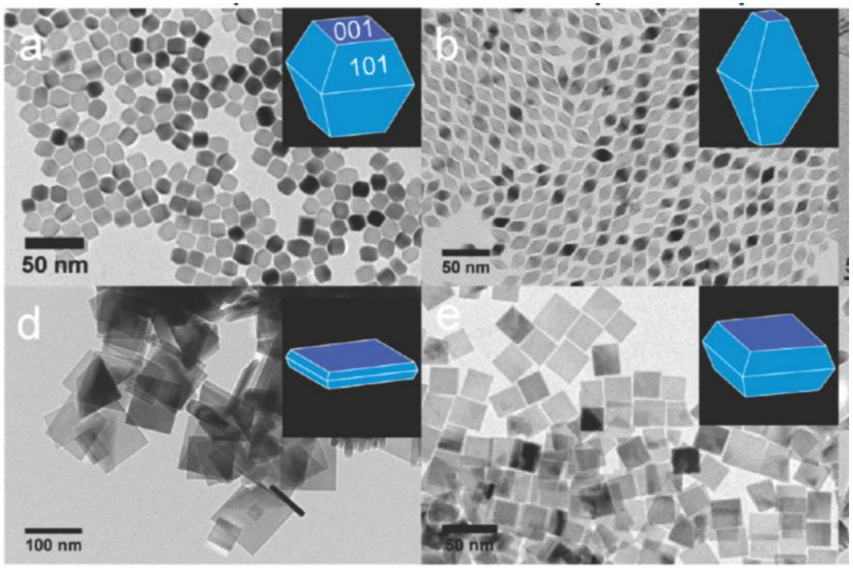

Industrial commercial NPs

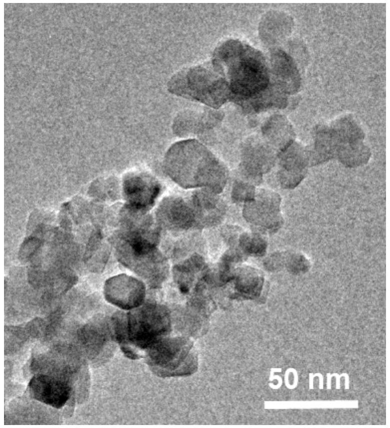

TiO_2 P25 (Evonik)

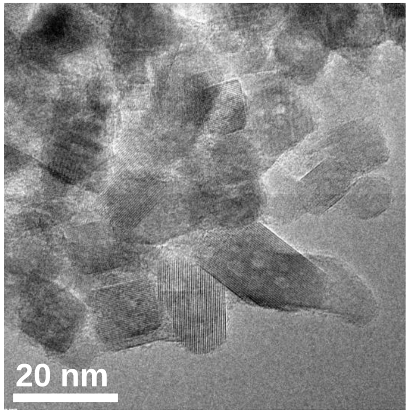

TiO_2 T-SP (Solaronix)

In «real» commercial samples the NPs heterogeneity often makes the extraction of statistically significant information from TEM images laborious and subject to bias

Combining scattering and spectroscopy

Study ot the crystallization process from amorphous TiO_2 to anatase

Ti K-edge XAS

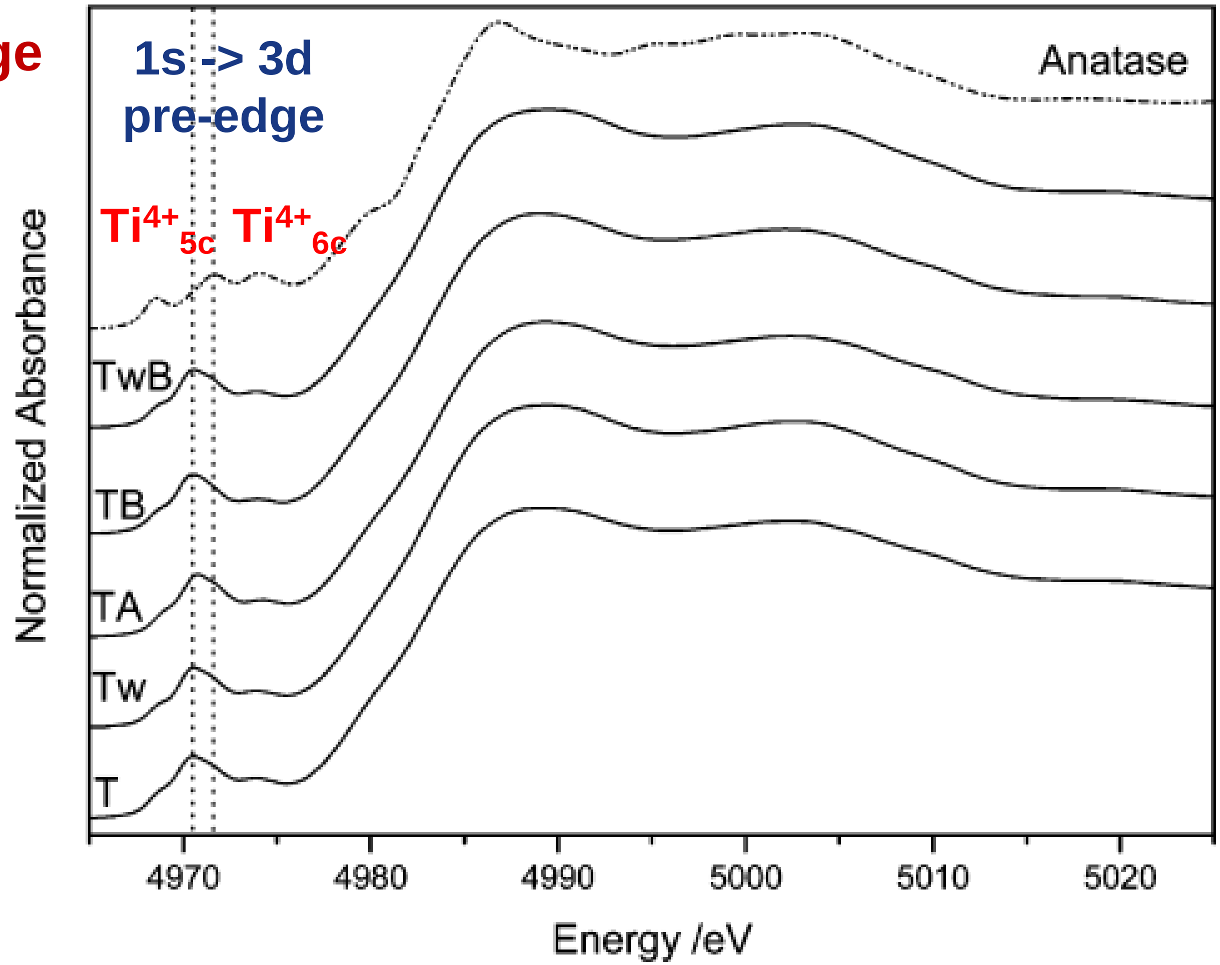

M. Fernandez-Garcia et al., J. Am. Chem. Soc. 2007, 129, 13604 - 13612

XANES highlights the presence of Ti^{4+}_{5c} in amorphous TiO_2.

Ti K-edge EXAFS analysis

M. Fernandez-Garcia et al., J. Am. Chem. Soc. 2007, 129, 13604 - 13612

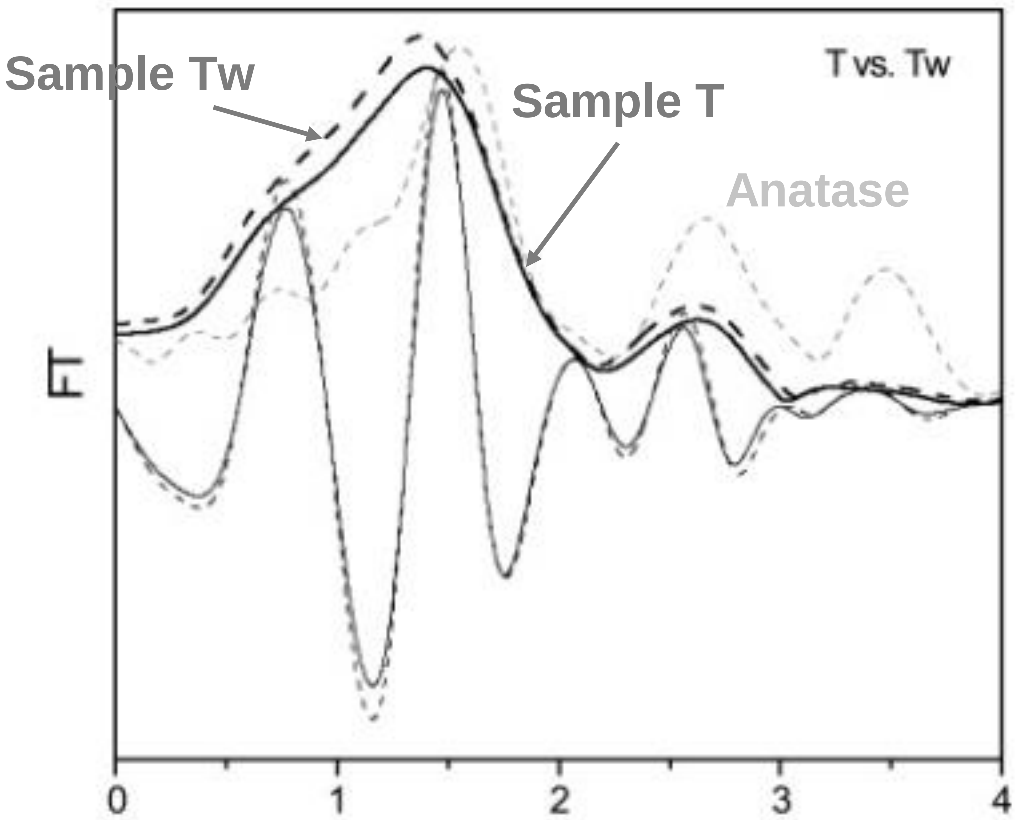

shell	N	R/Å	$\Delta\sigma/10^3 \times Å^2$
		T; 7.7%[a]	
Ti−O	$1.2_5 \pm 0.3_5$	1.72 ± 0.02	10.1 ± 0.4
Ti−O	5.1 ± 0.6	1.91 ± 0.01	7.5 ± 0.7
Ti−Ti	1.9 ± 0.3	3.02 ± 0.01	2.0 ± 0.6
		Tw; 8.9%	
Ti−O	$1.4_5 \pm 0.4$	1.73 ± 0.02	9.0 ± 0.5
Ti−O	5.3 ± 0.7	1.90 ± 0.01	8.5 ± 0.6
Ti−Ti	2.2 ± 0.3	3.03 ± 0.01	1.7 ± 0.6
		TA, 11.1%	
Ti−O	$1.2_5 \pm 0.3_5$	1.72 ± 0.02	9.5 ± 0.3
Ti−O	5.0 ± 0.7	1.90 ± 0.01	7.0 ± 0.7
Ti−Ti	$2.3 \pm 0.3_5$	3.04 ± 0.01	1.5 ± 0.8
		TB; 8.7%	
Ti−O	1.3 ± 0.3	1.72 ± 0.02	9.0 ± 0.3
Ti−O	5.1 ± 0.7	1.90 ± 0.01	7.0 ± 0.5
Ti−Ti	2.2 ± 0.3	3.02 ± 0.01	2.4 ± 0.8
		TwB; 5.7%	
Ti−O	$1.4 \pm 0.3_5$	1.74 ± 0.02	9.1 ± 0.4
Ti−O	5.3 ± 0.7	1.92 ± 0.01	8.0 ± 0.4
Ti−Ti	2.6 ± 0.3	3.05 ± 0.01	1.0 ± 0.9

Low Ti - Ti coordination numbers (for crystalline anatase CN = 4) suggests that Ti cations have a severely restricted 3D connectivity in all samples.

In situ XRD patterns during heating

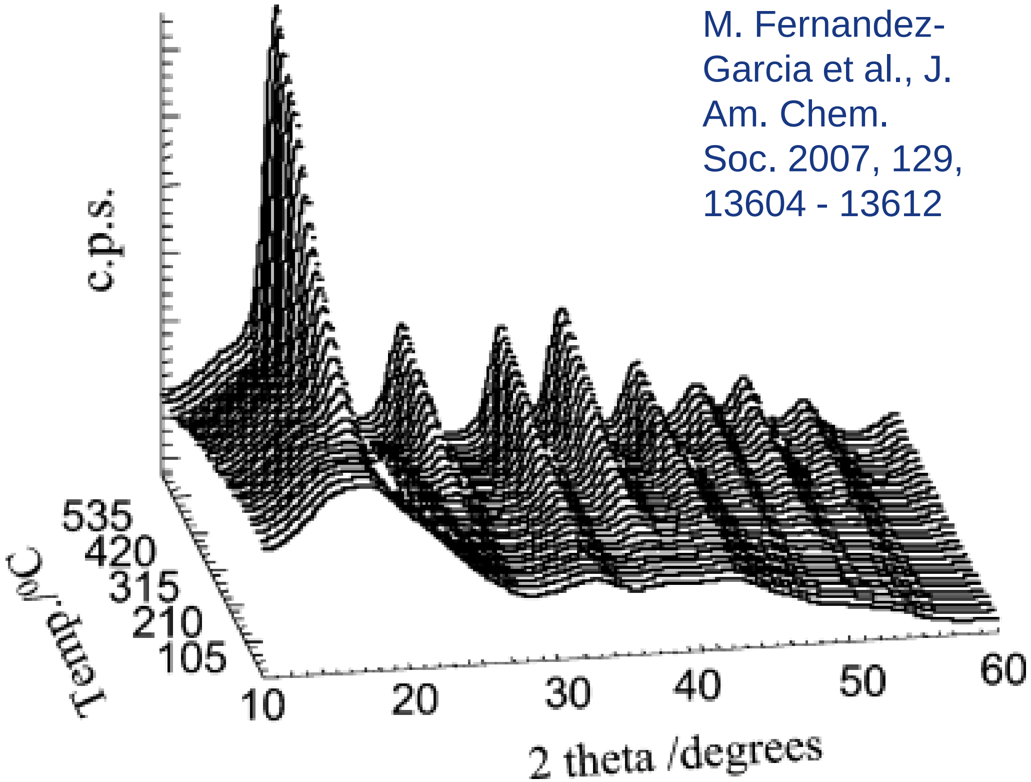

M. Fernandez-Garcia et al., J. Am. Chem. Soc. 2007, 129, 13604 - 13612

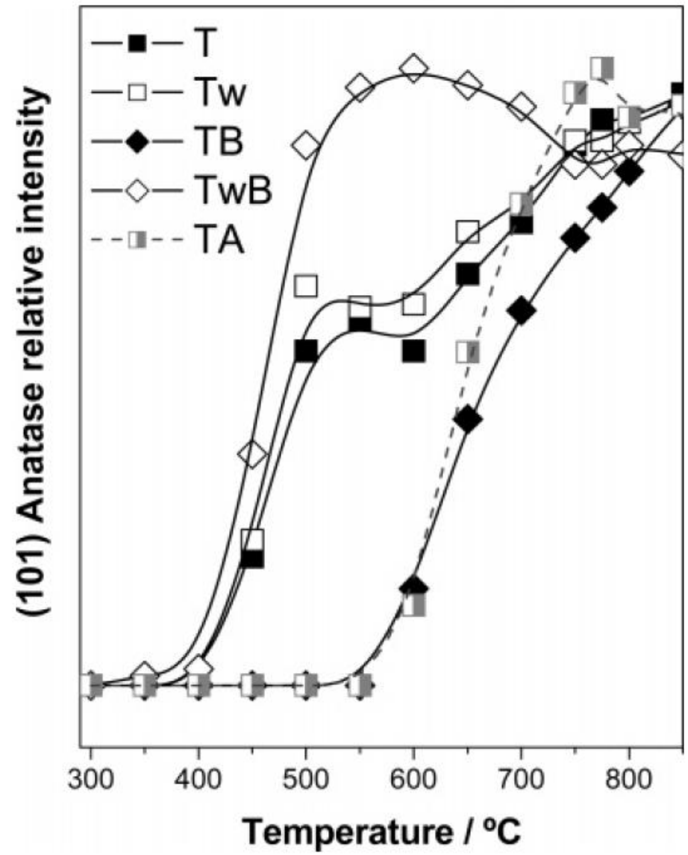

Upon heating in dry air, samples T, Tw, and TwB nucleate around 350 - 400 ˚C, samples TA and TB nucleate around 550 ˚C

Monitoring crystallization by PDF

PDF obtained during heating in dry air in step of 50 ˚C

Sample T

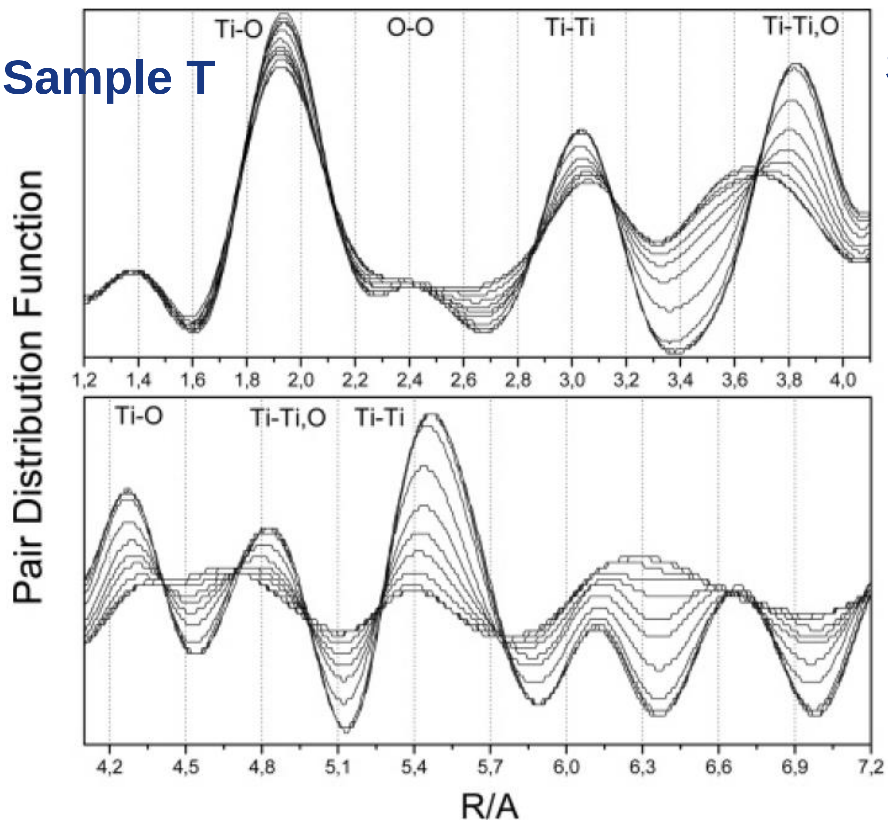

Sample TA

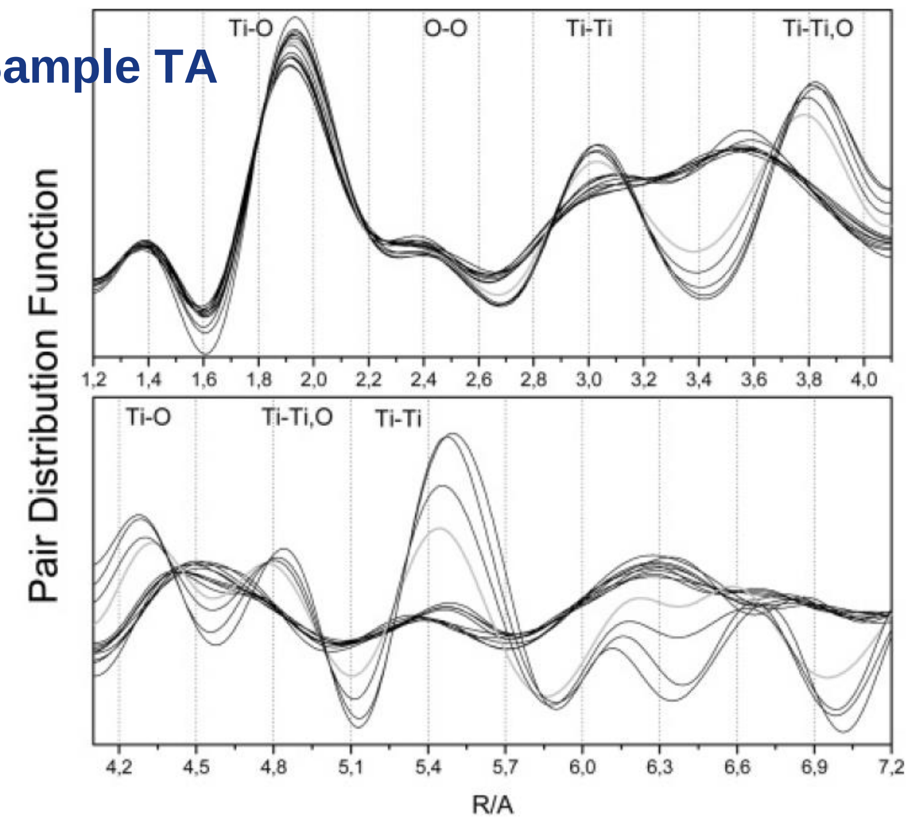

Crystallization onset temperature is clearly related to the local middle range order (3 - 4 Å) of the different samples

Let's complicate a little bit the system…

Supported metal NPs

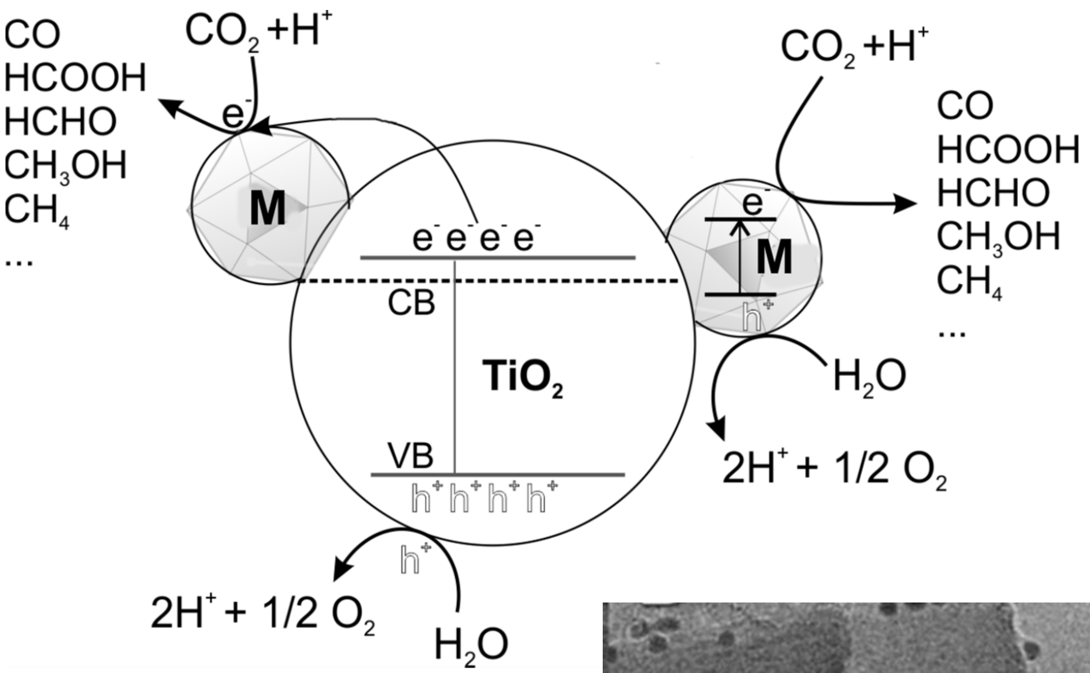

Increase electron-hole lifetime

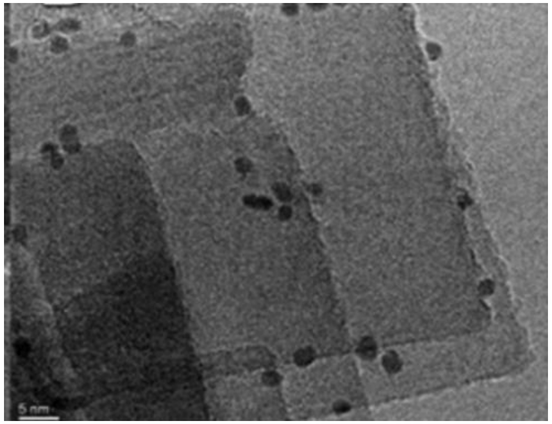

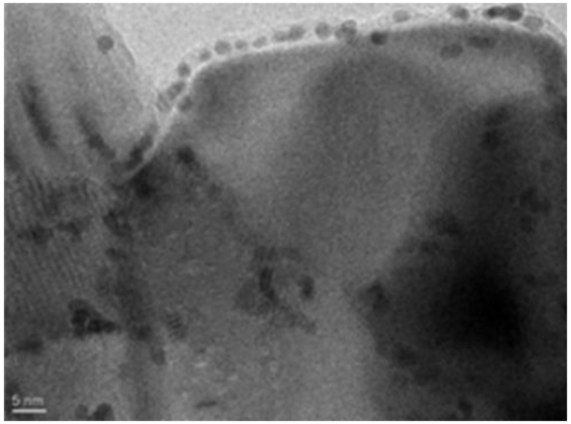

F. Pellegrino et al., ACS Catal.. 2019, 129, 13604 - 13612

Pt NPs photodeposition

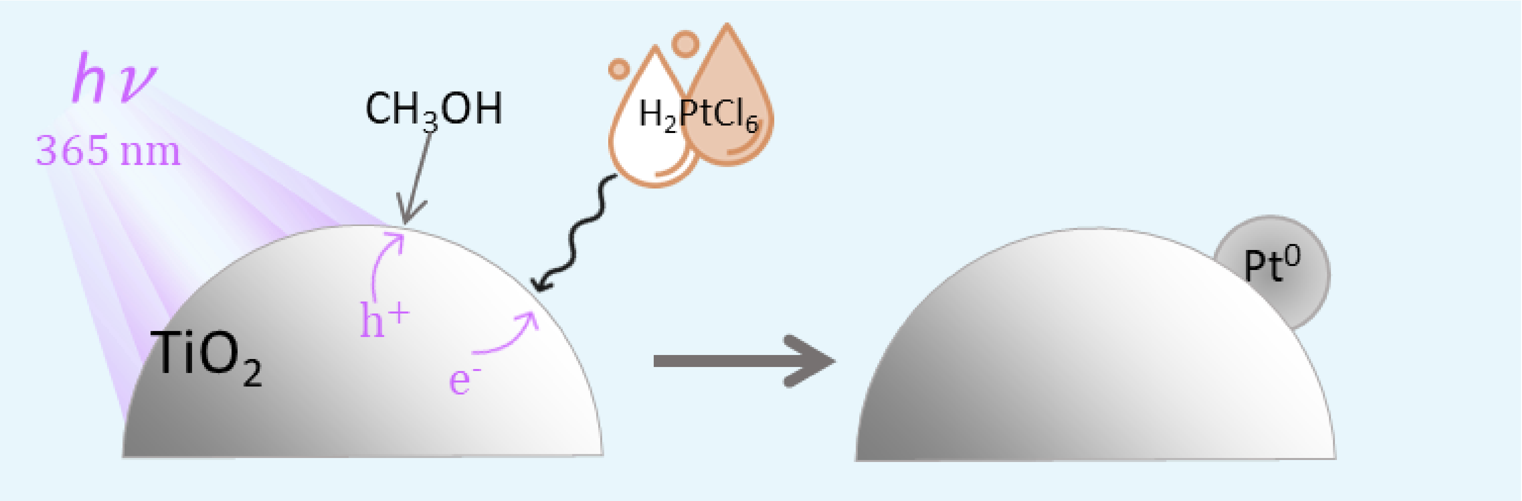

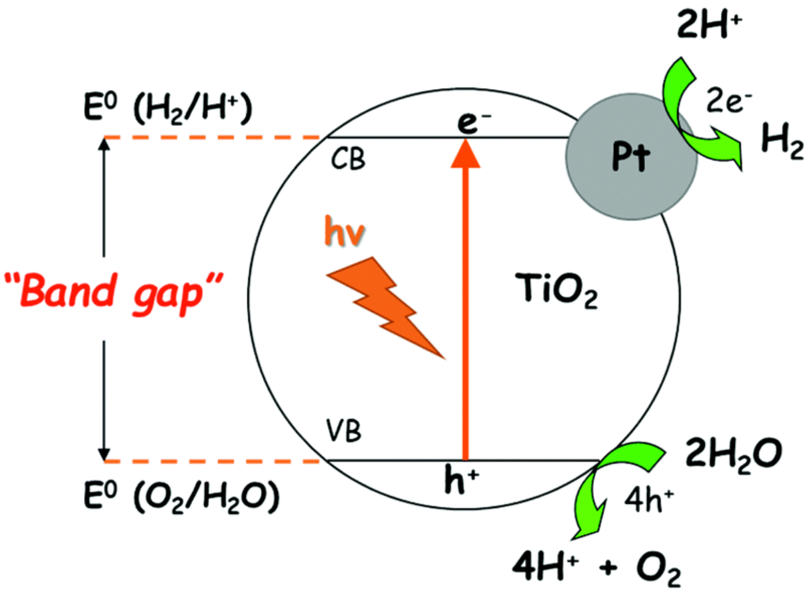

Hydrogen production from water

XAS *operando* setup

3D-printed *operando* photocatalytic cell

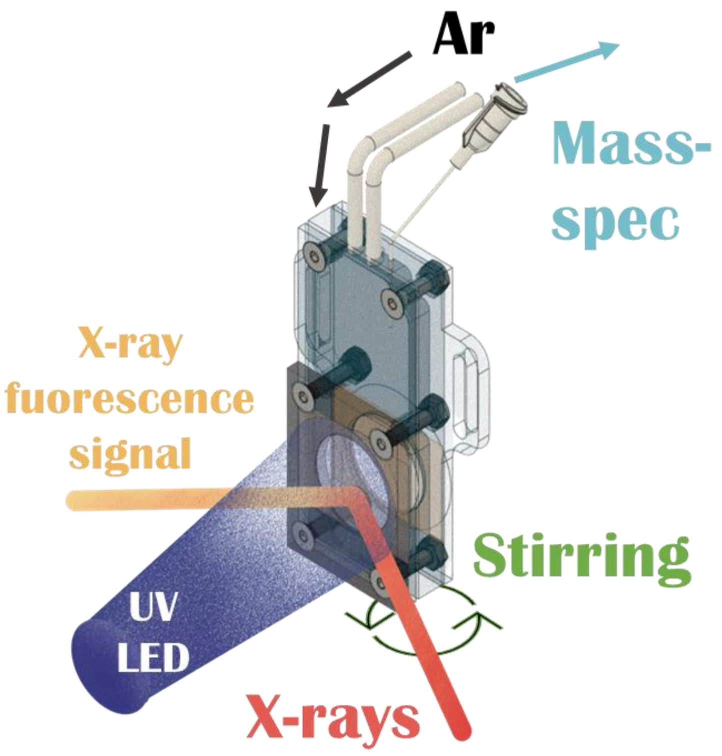

E. Kozyr et al. Catalysts (2023) 13, 414

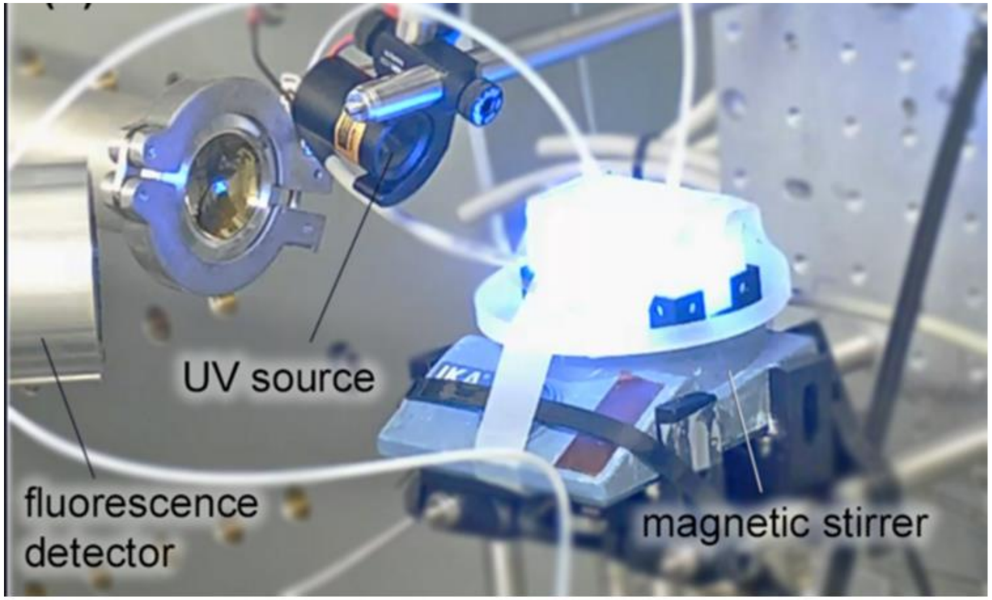

E. Kozyr et al. J. Synchrotron Rad. (2024) 31, 1071–1077

XAS Pt L_3-edge: study of photodeposition

ESRF BM23 beamline

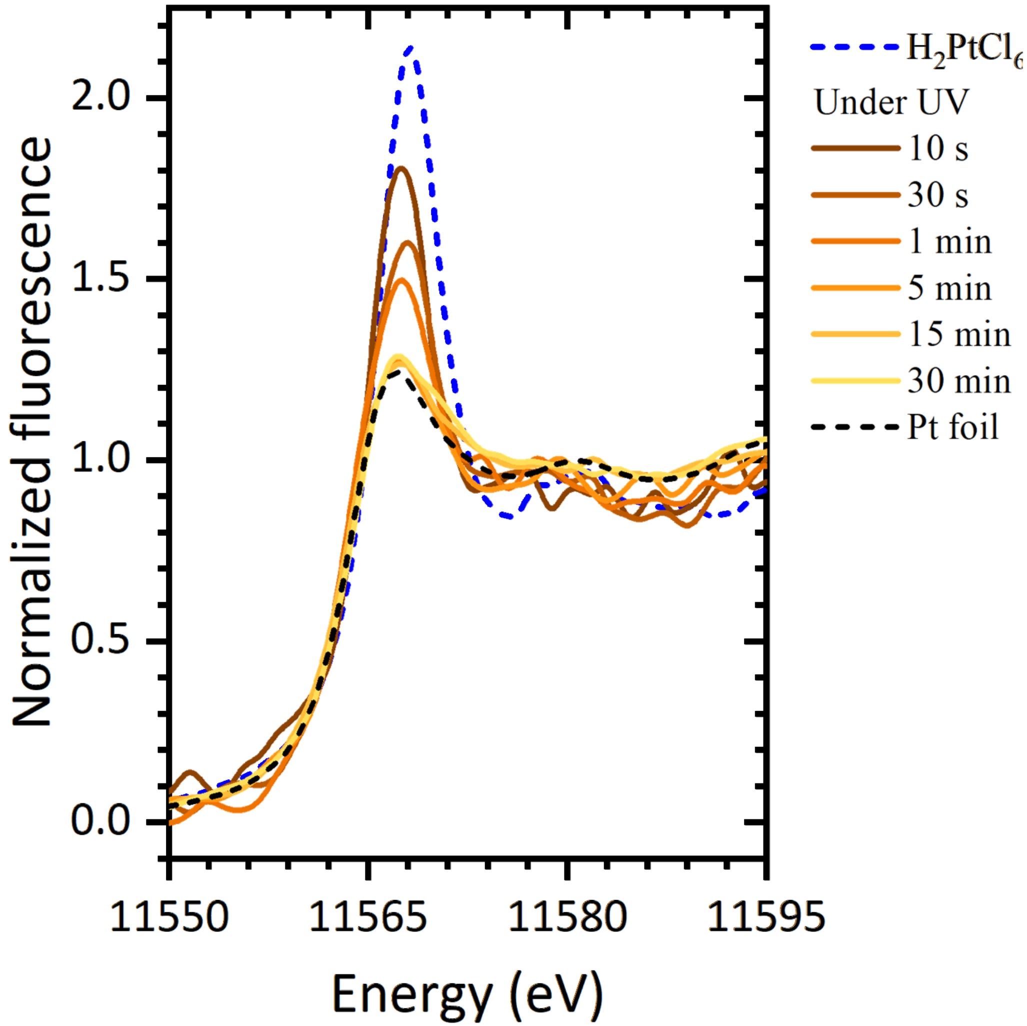

TiO_2

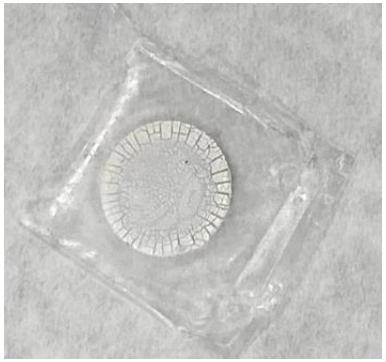

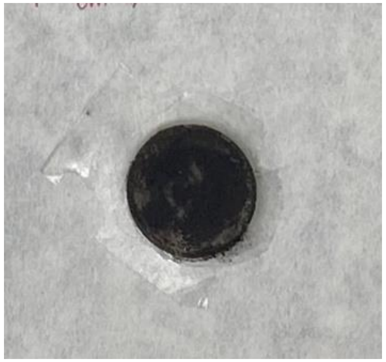

Pt/TiO_2

XAS *operando* study of H_2 photoproduction

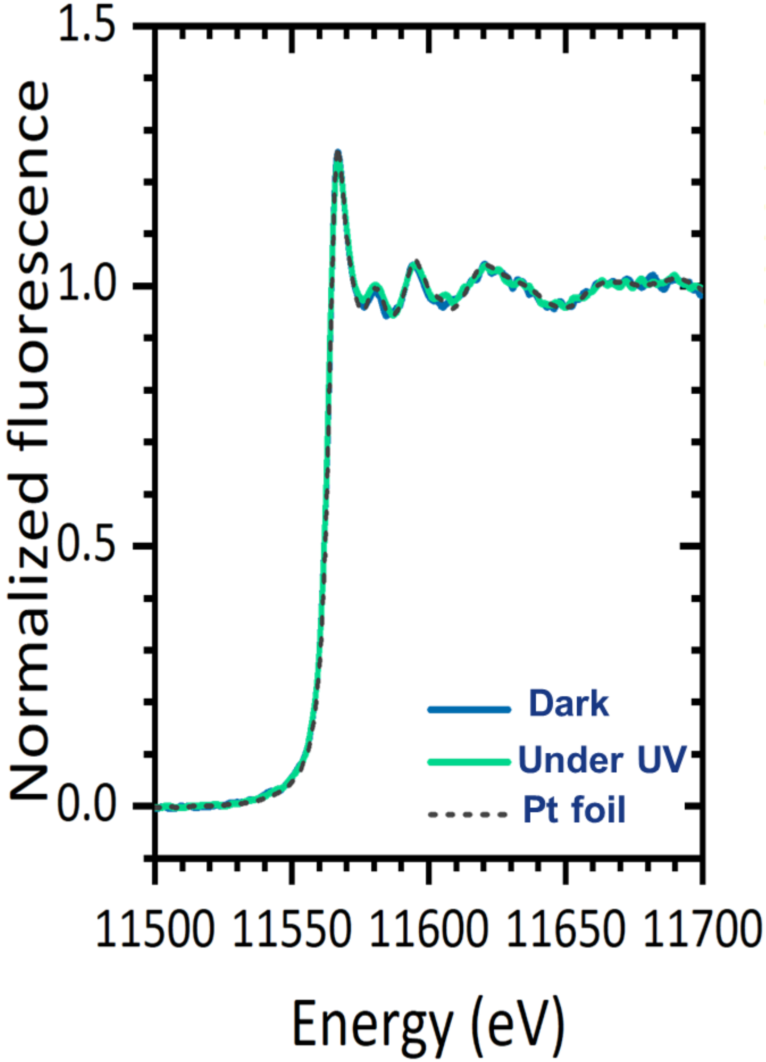

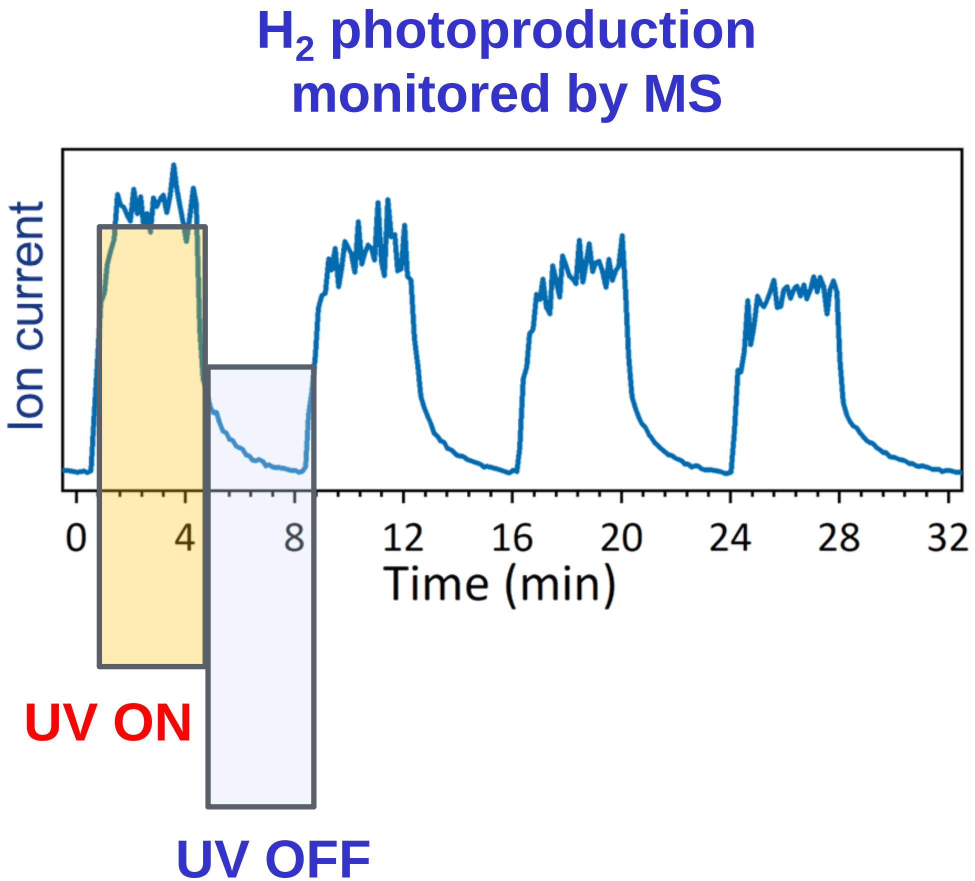

Photocatalytic H_2 production

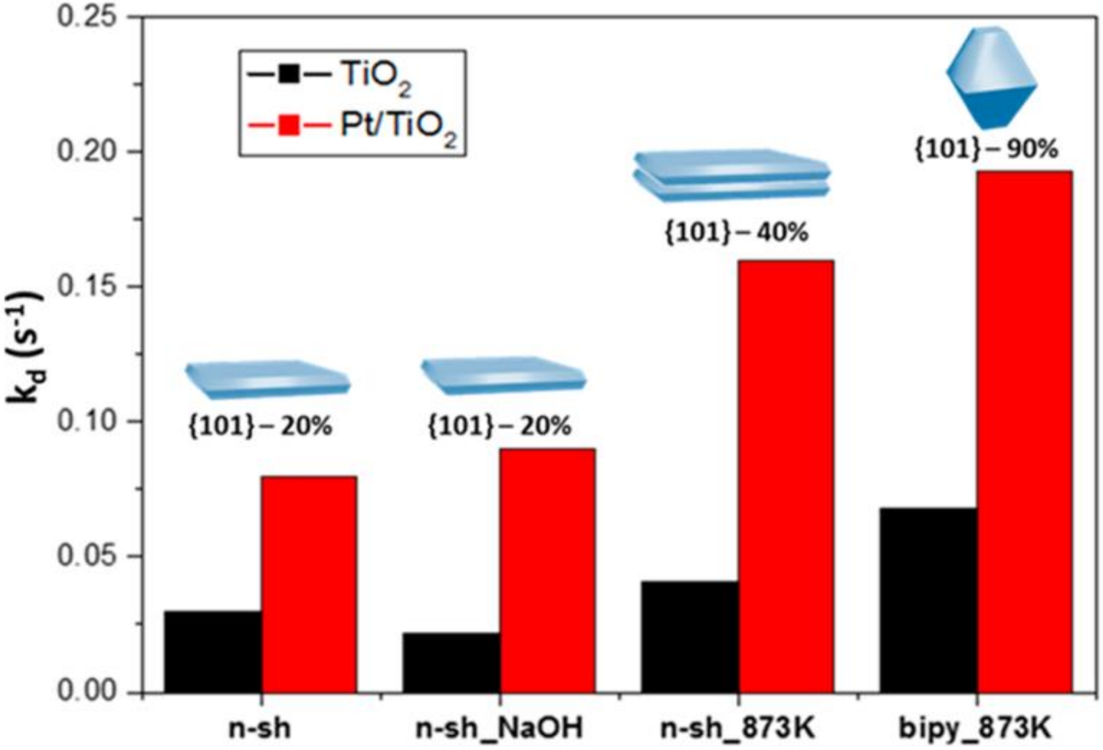

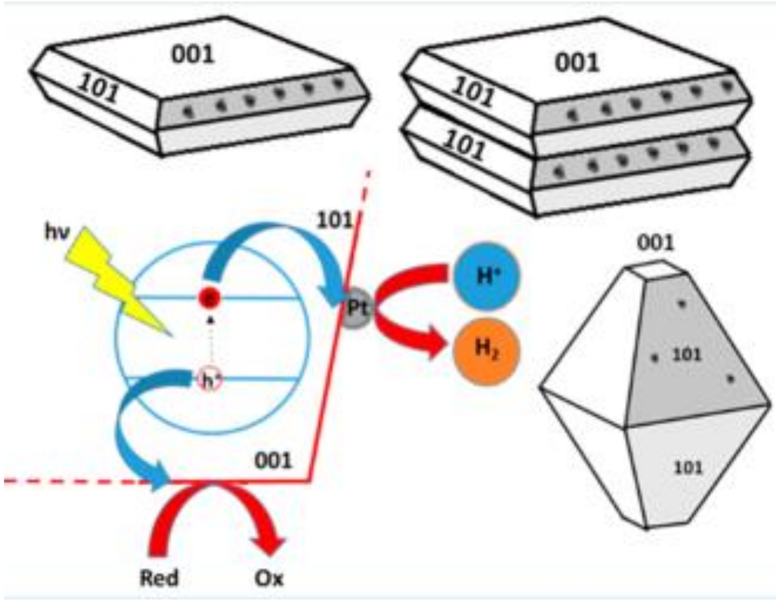

F. Pellegrino et al., ACS Catal.. 2019, 129, 13604 - 13612

Let’s jump to a more complex case: real devices…

Nanostructured device characterization

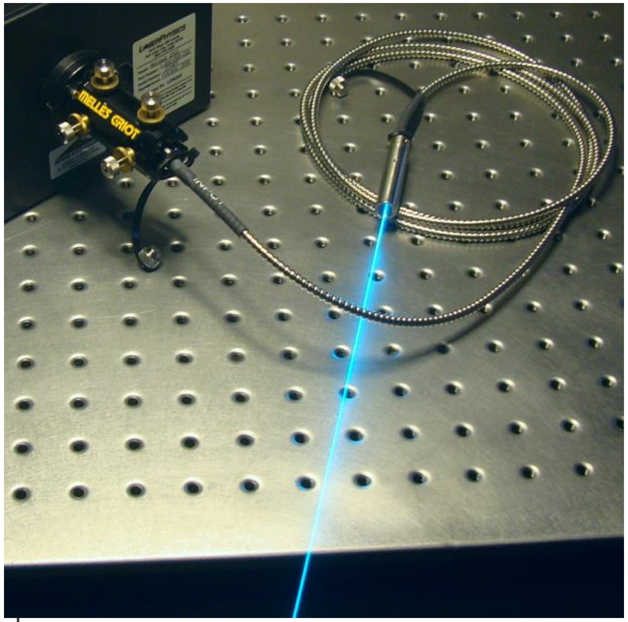

Semiconductor nanostructures to realize lasers and modulators for fiber-optics communications

Both laser and modulator are $In_xGa_yAl_{1-x-y}As$ multi quantum well (MQW) heterostructures grown on InP(001)

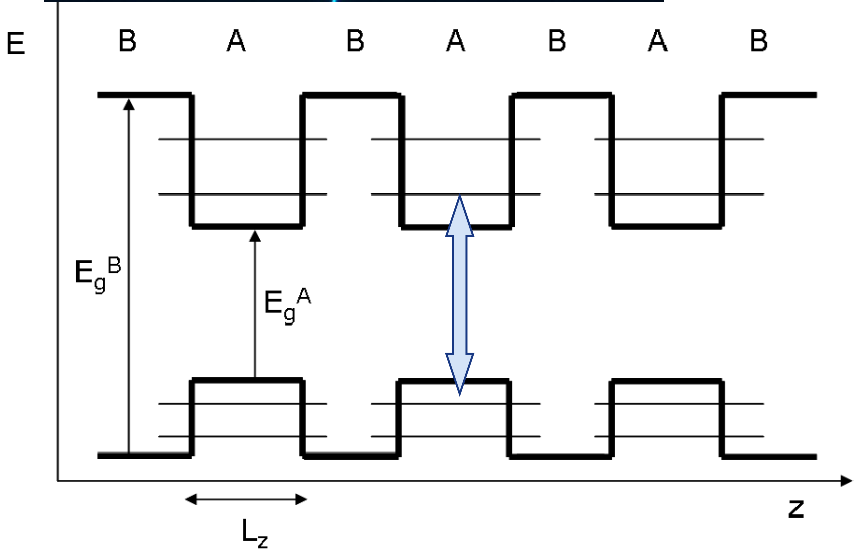

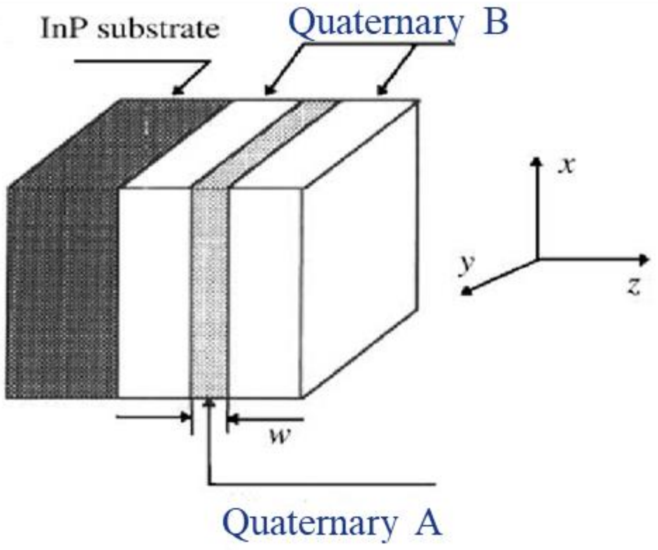

Signal modulation for fiber-optic communication

The signal can be modulated in two different ways:

- **Direct**: modulating the laser current

non equilibrium in the charge carriers causes frequency shifts in the emitted radiation

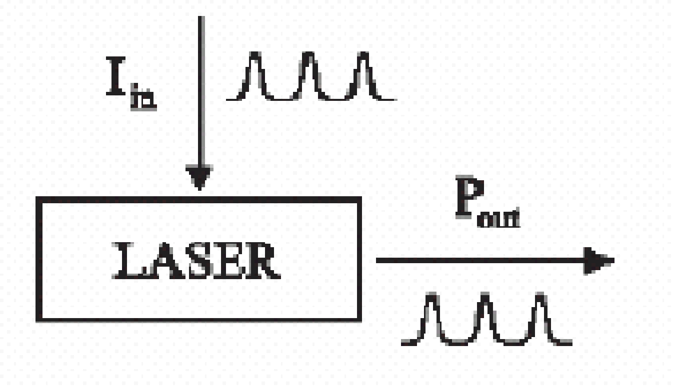

- **External:** two different devices act as laser source and signal modulator

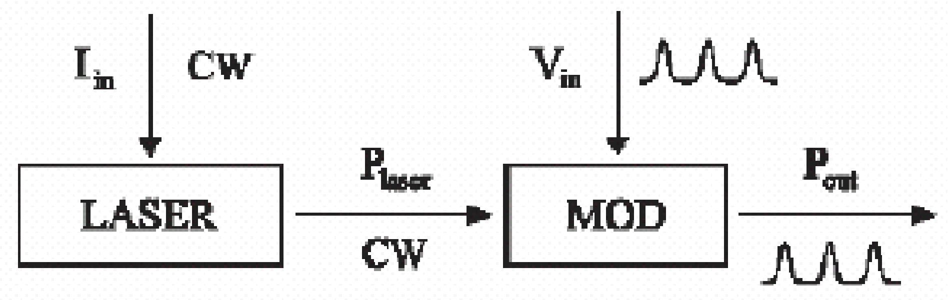

both the frequency (Gbit/s) and transmission lengths are improved

Electro-absorption modulator (EAM)

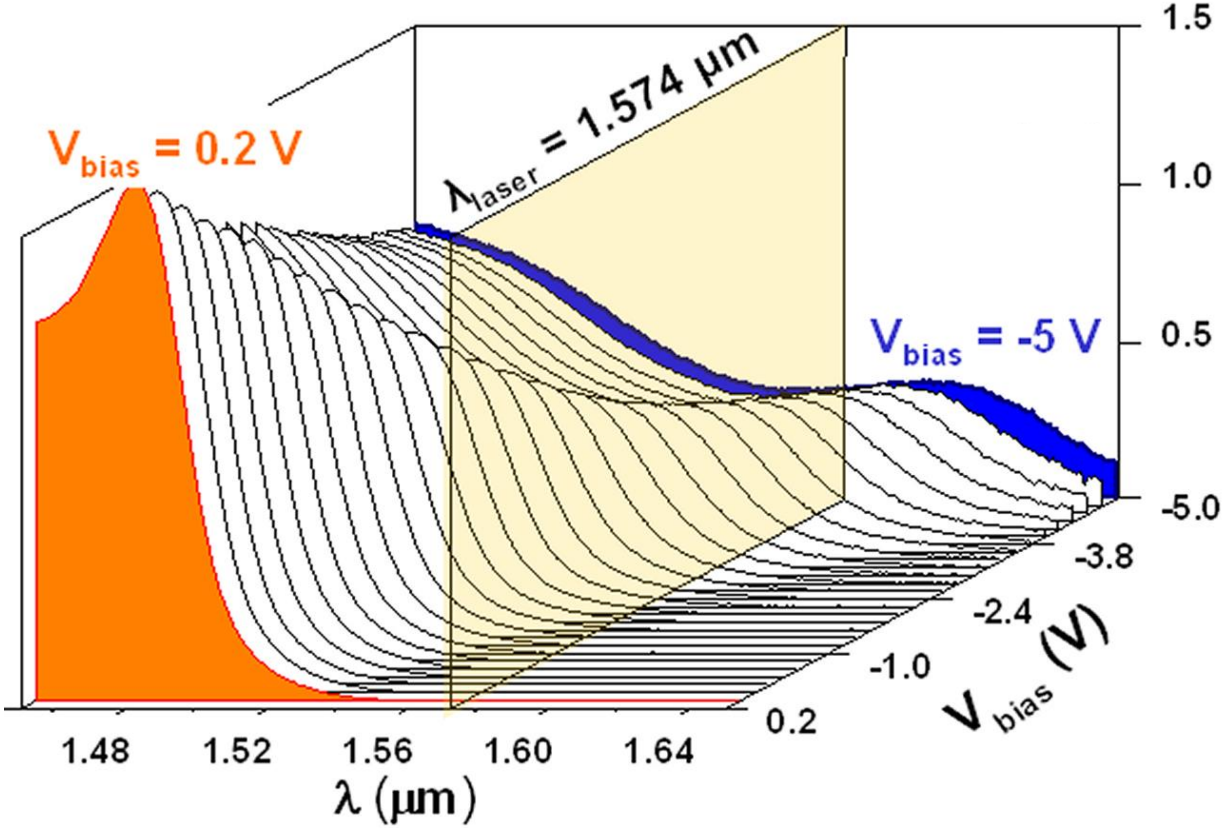

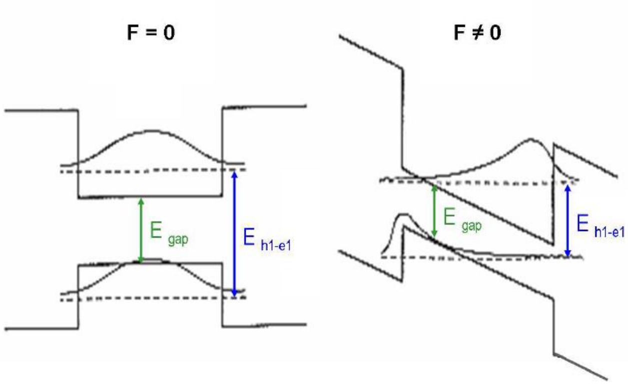

L. Mino et al., Small 2011, 7, 930-938

A suitable voltage switches the EAM from transparent to opaque (Stark effect)

Modulator (EAM)- DFB laser inte

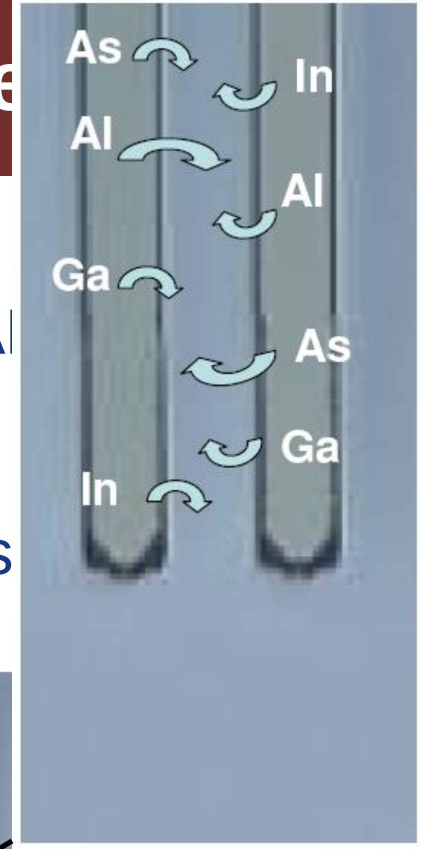

Monolithic integration of the laser and the EA

⇩

Selective Area Growth (SAG): a SiO_2 mas
the precursors flux

⇩

variation in composition and thickness of the material grown between the SiO_2 stripes

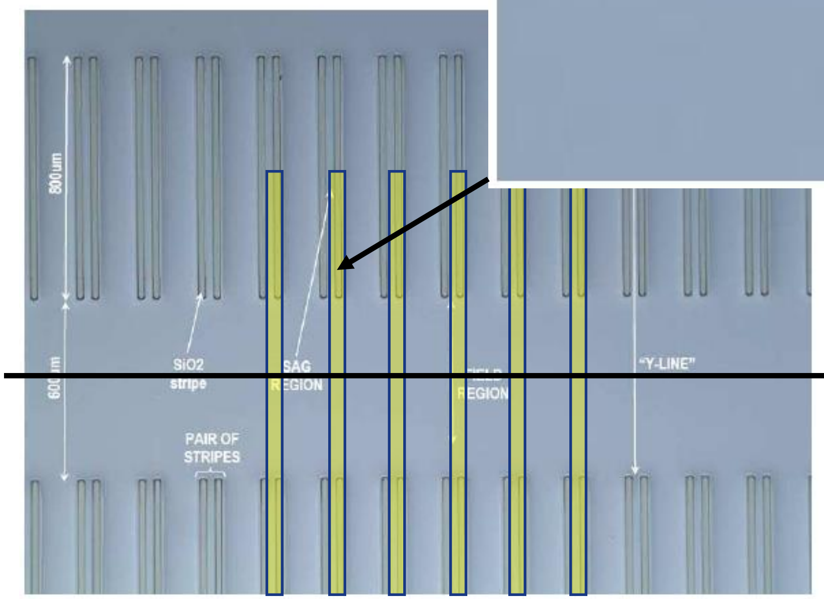

The complete modulator-laser device

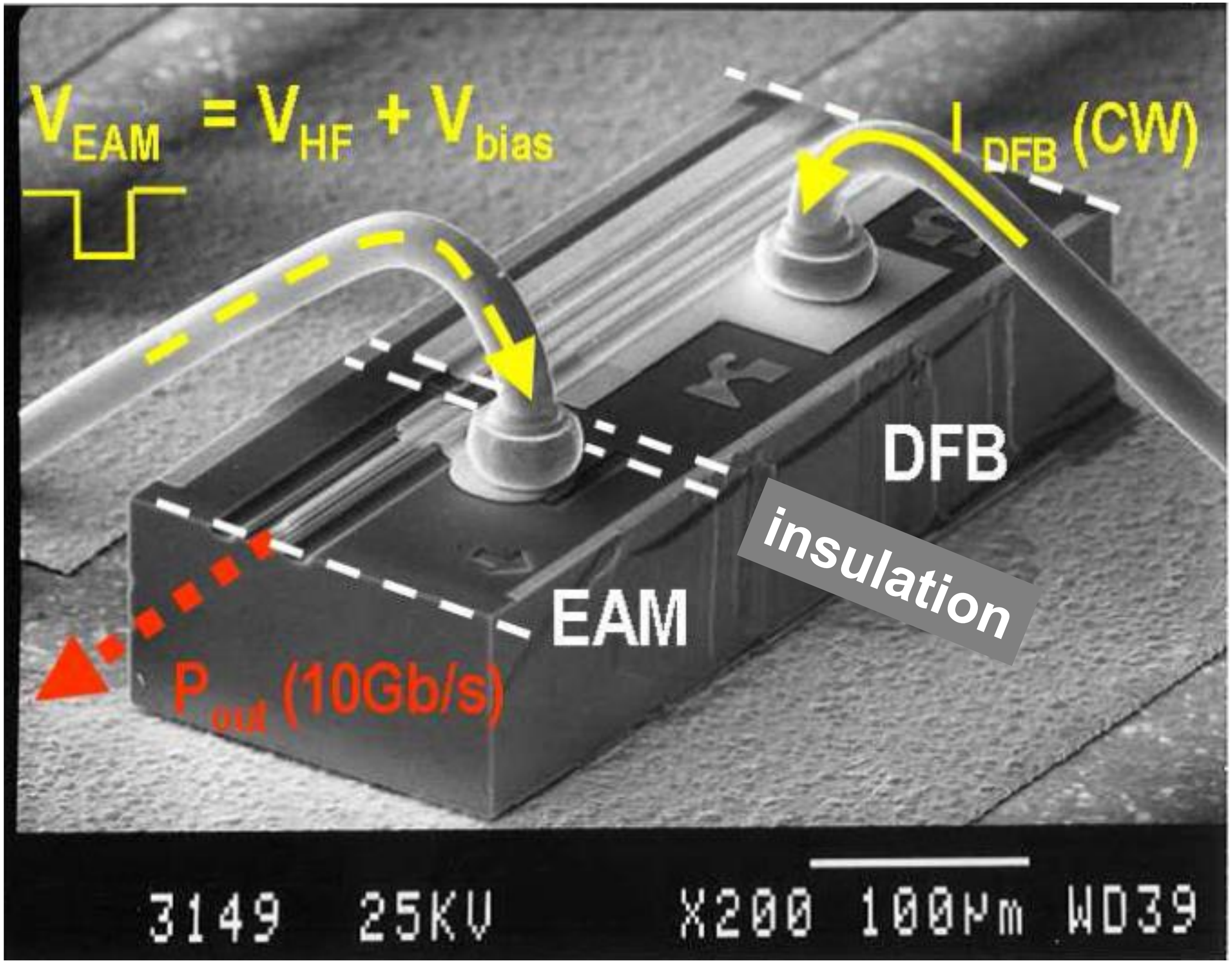

Energy gap space-resolved determination

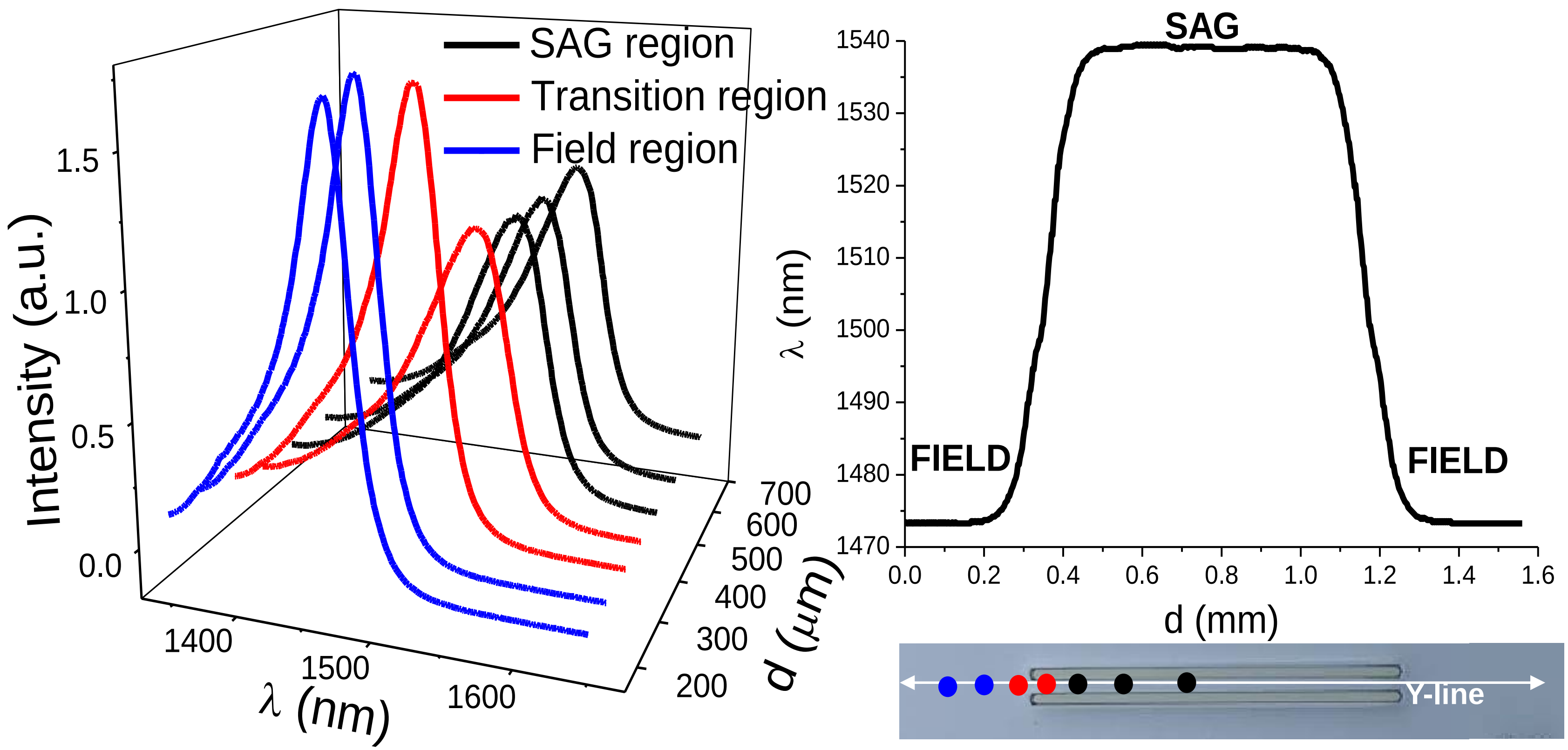

Space resolved photoluminescence (PL) study with a 15 μm resolution along a line parallel to the SiO_2 stripes (Y-line)

L. Mino et al., Adv. Mater. 2010, 22, 2050-2054

Energy gap space-resolved determination

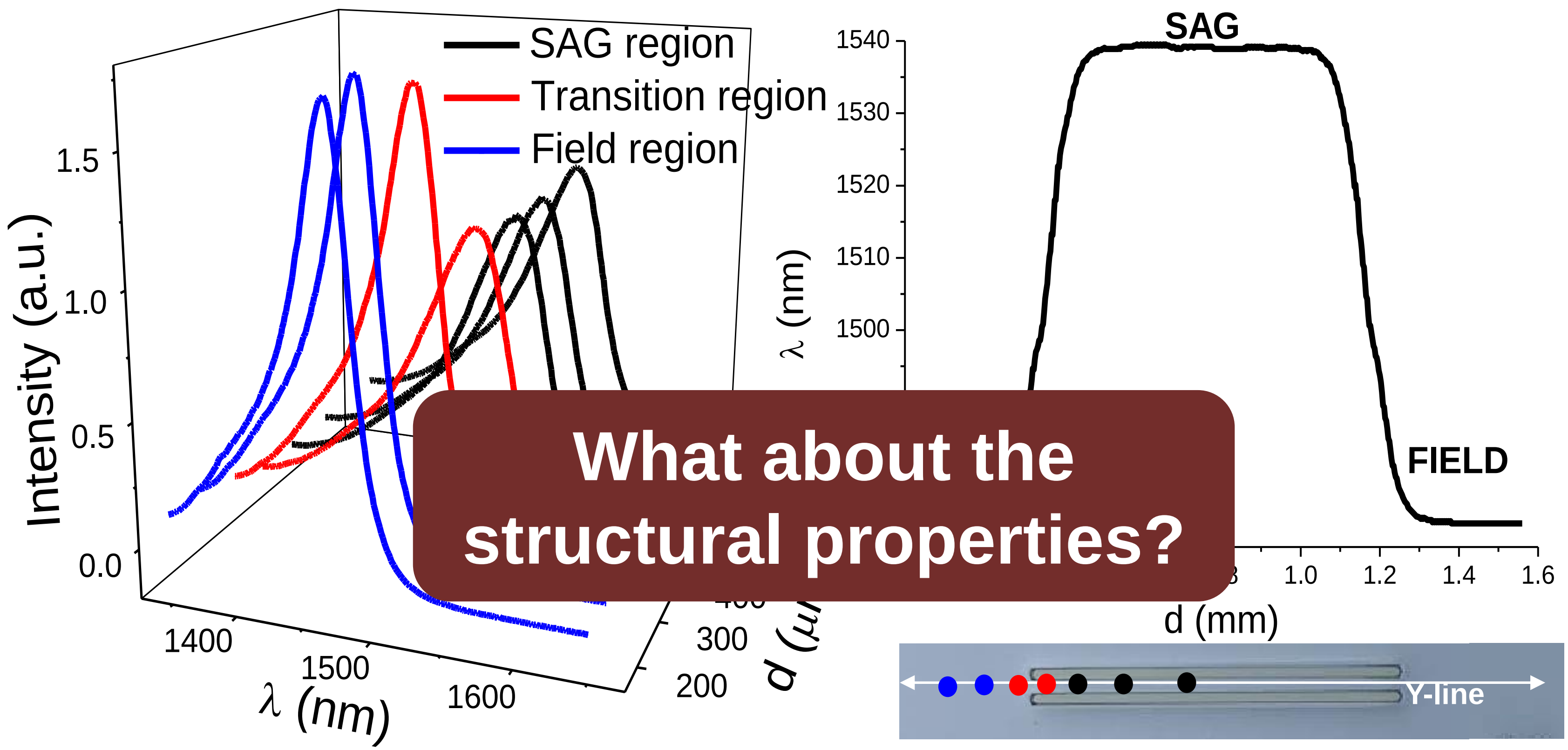

What about the structural properties?

Space resolved photoluminescence (PL) study with a 15 μm resolution along a line parallel to the SiO_2 stripes (Y-line)

L. Mino et al., Adv. Mater. 2010, 22, 2050-2054

Synchrotron X-ray micro-/nano-beams

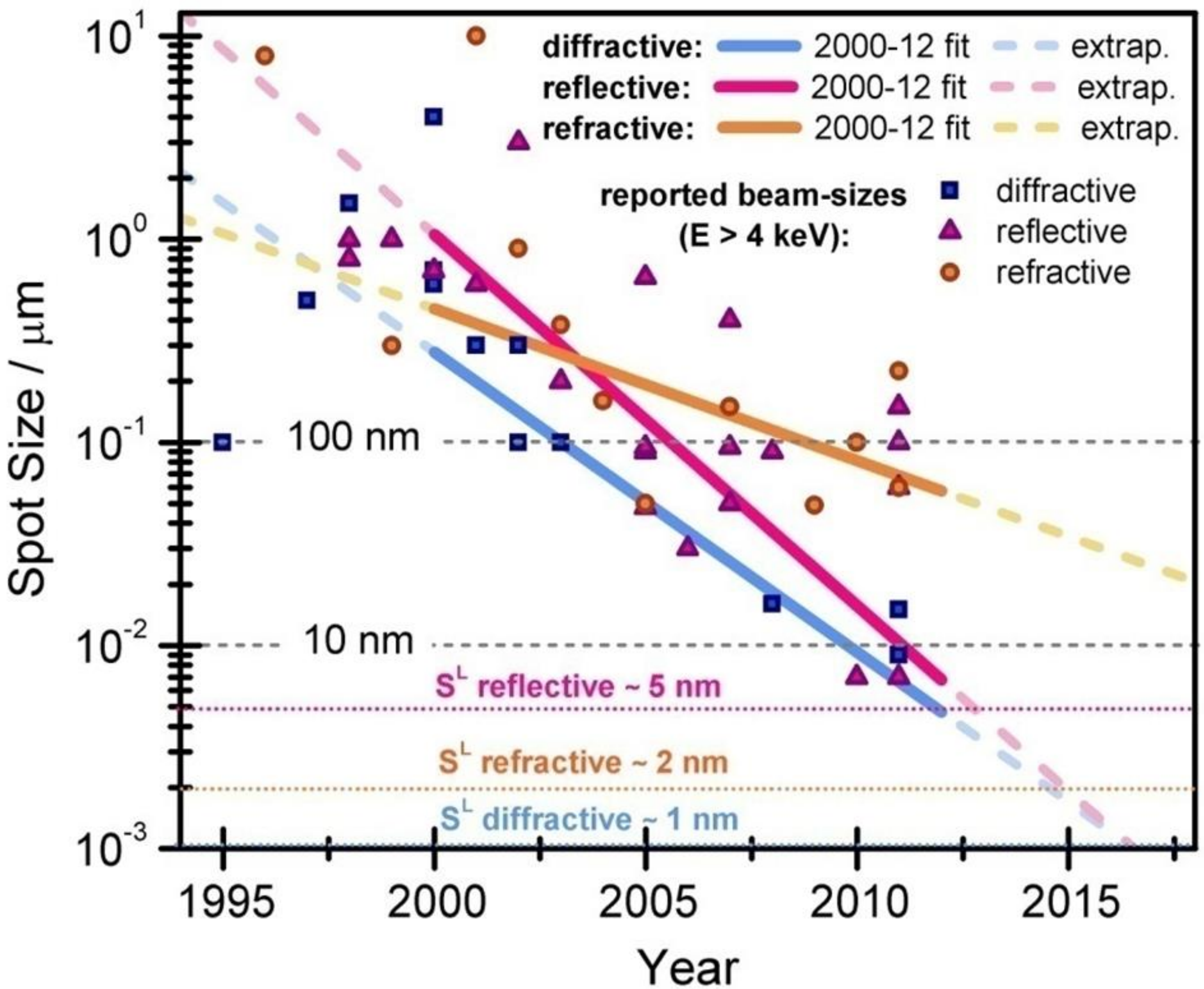

L. Mino et al., Rev. Mod. Phys. 2018, 90, 025007

ESRF ID22 beamline (now ID16)

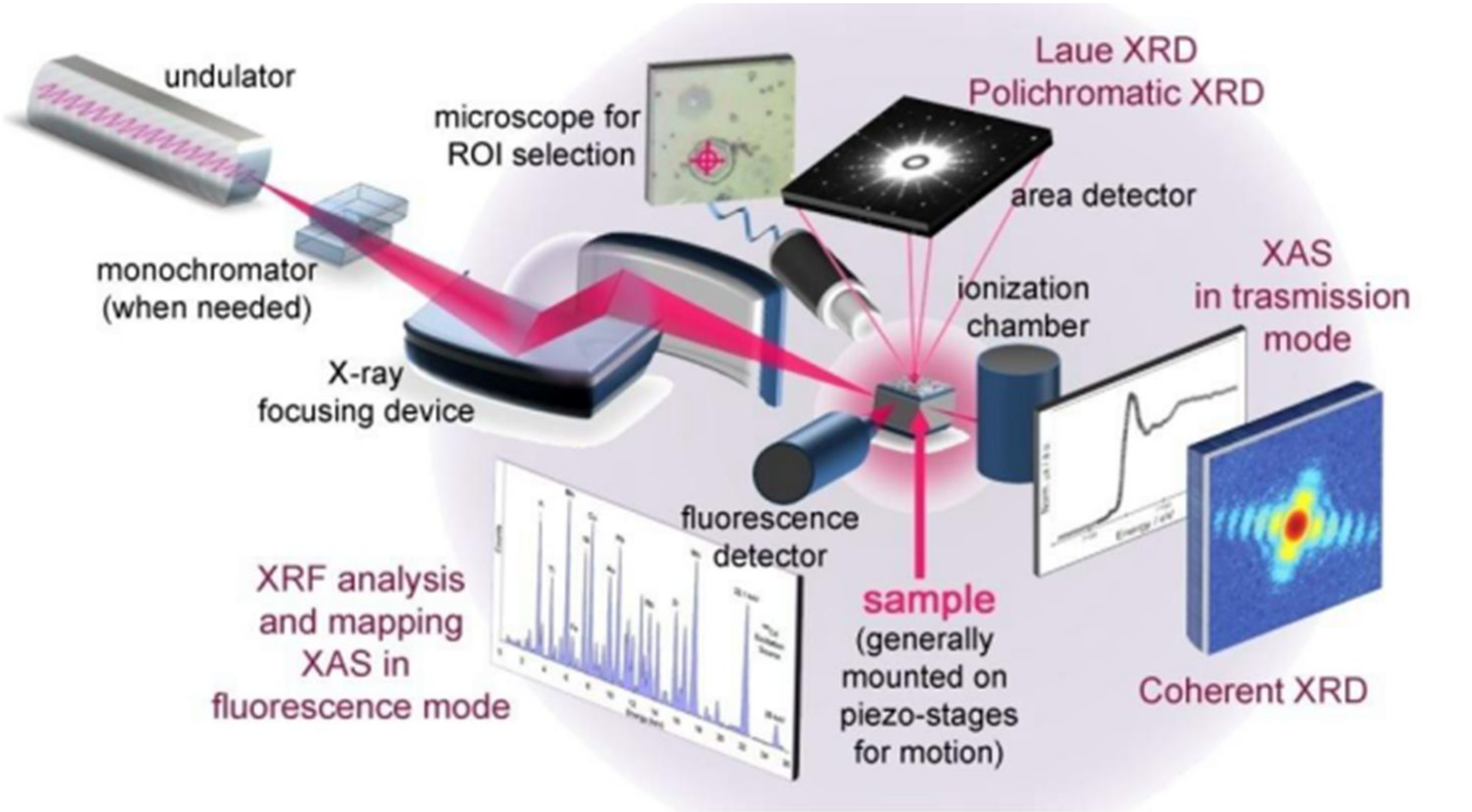

X-ray micro-beam: 1.7 μm × 5.3 μm

Micro-XRD experimental setup

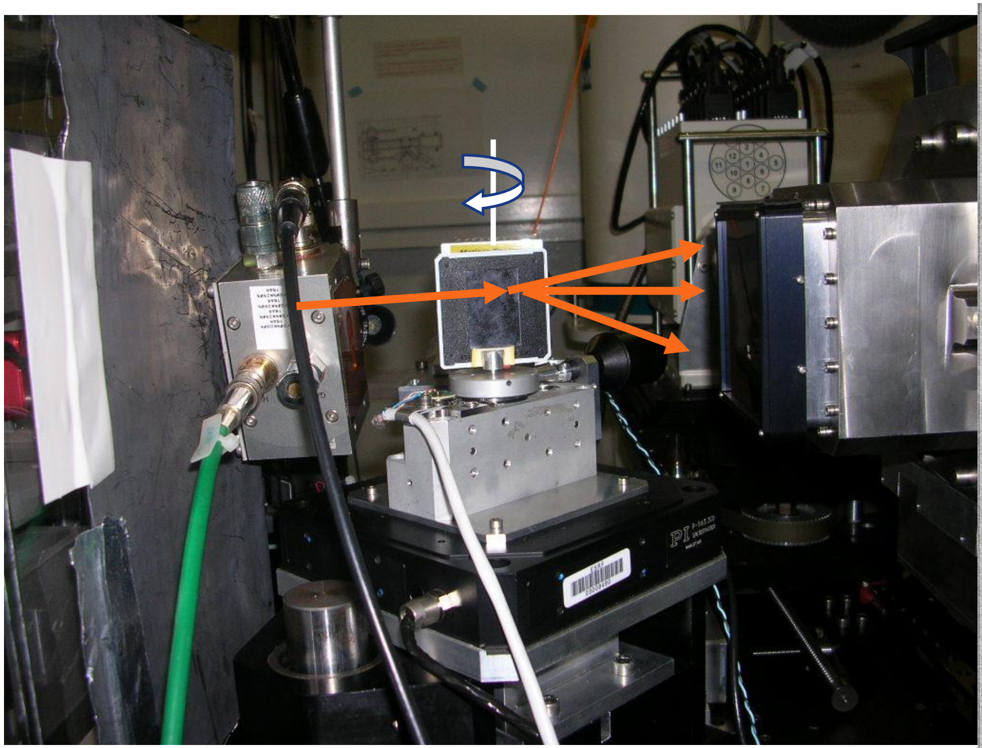

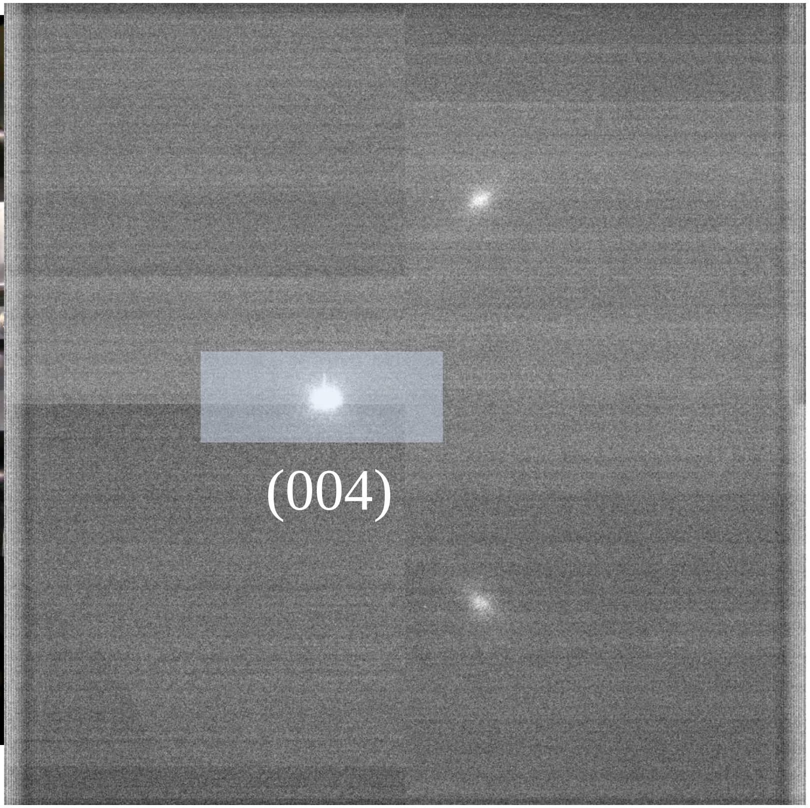

CCD image

Micro-XRD pattern acquisition

176 images covering a rotation of ± 1.1° around the InP(004) Bragg angle (θ_B = 14.359° at 17 keV)

35 different points have been sampled along the Y-line with 2 µm resolution

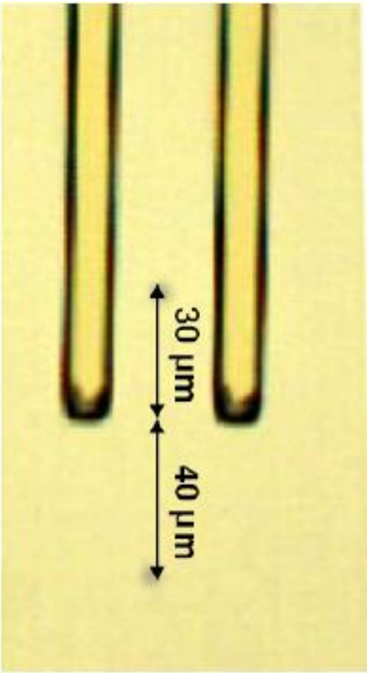

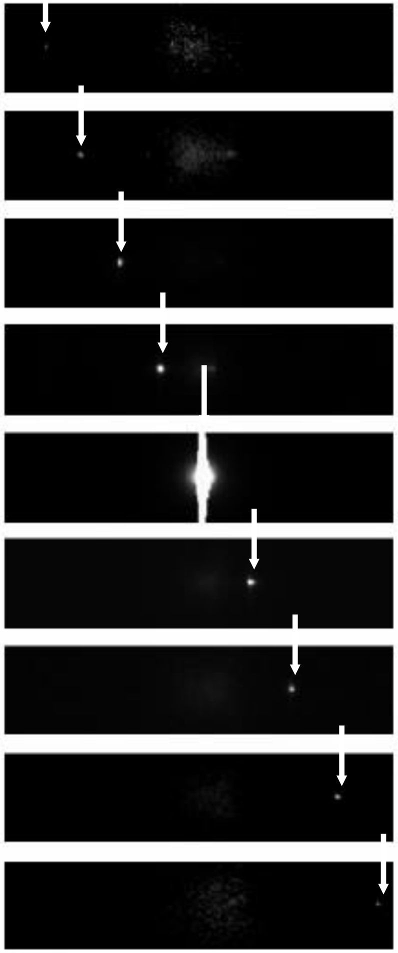

Reconstruction of the XRD patterns

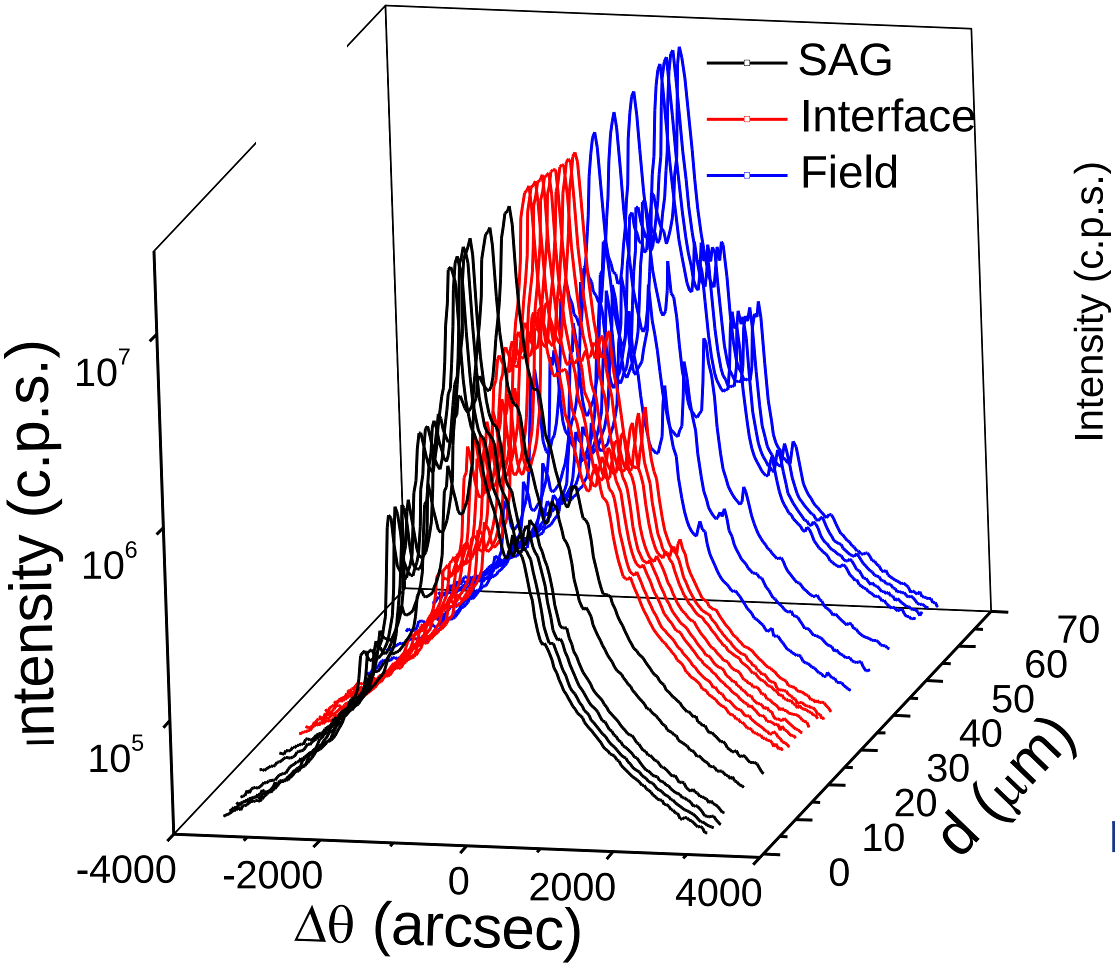

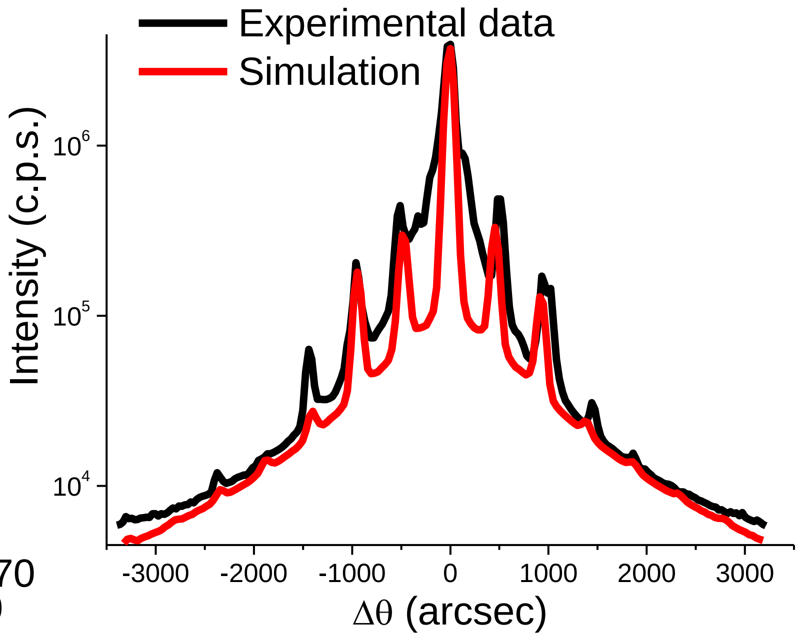

Each XRD pattern reconstructed starting from the 176 CCD images

L. Mino et al., Adv. Mater. 2010, 22, 2050-2054

Space-resoved XRD results

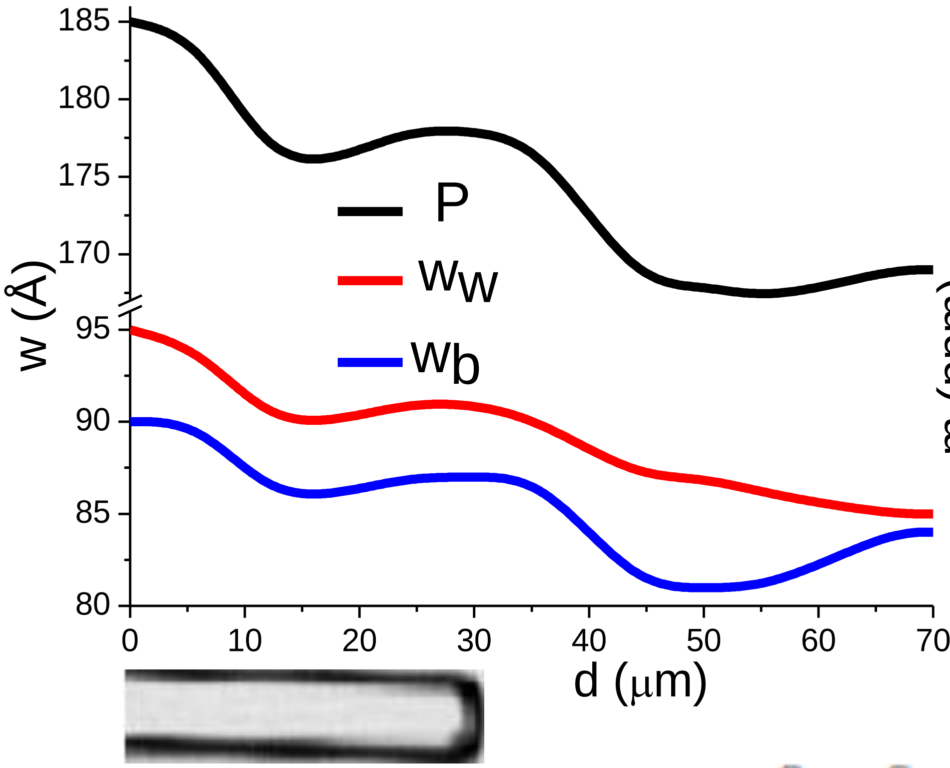

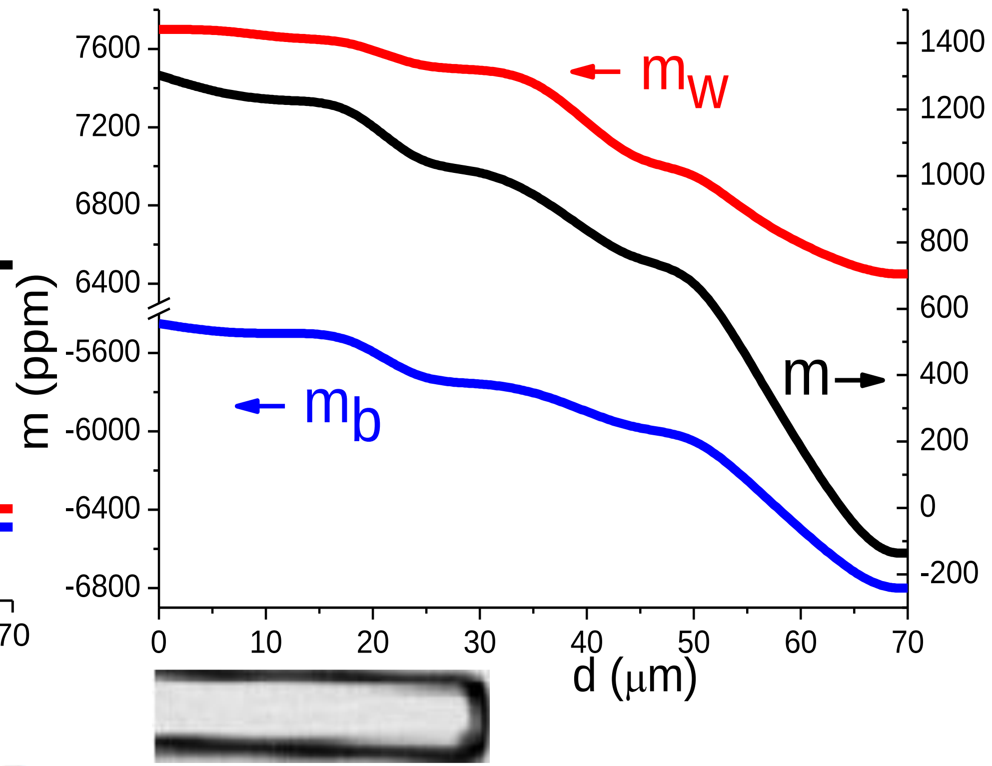

$$m = \frac{a - a_S}{a_S}$$

Widths (w_b, w_w) and mismatches (m_b, m_w) of the MQW barrier and of the well obtained performing a fitting of the XRD patterns

X-ray absorption spectroscopy

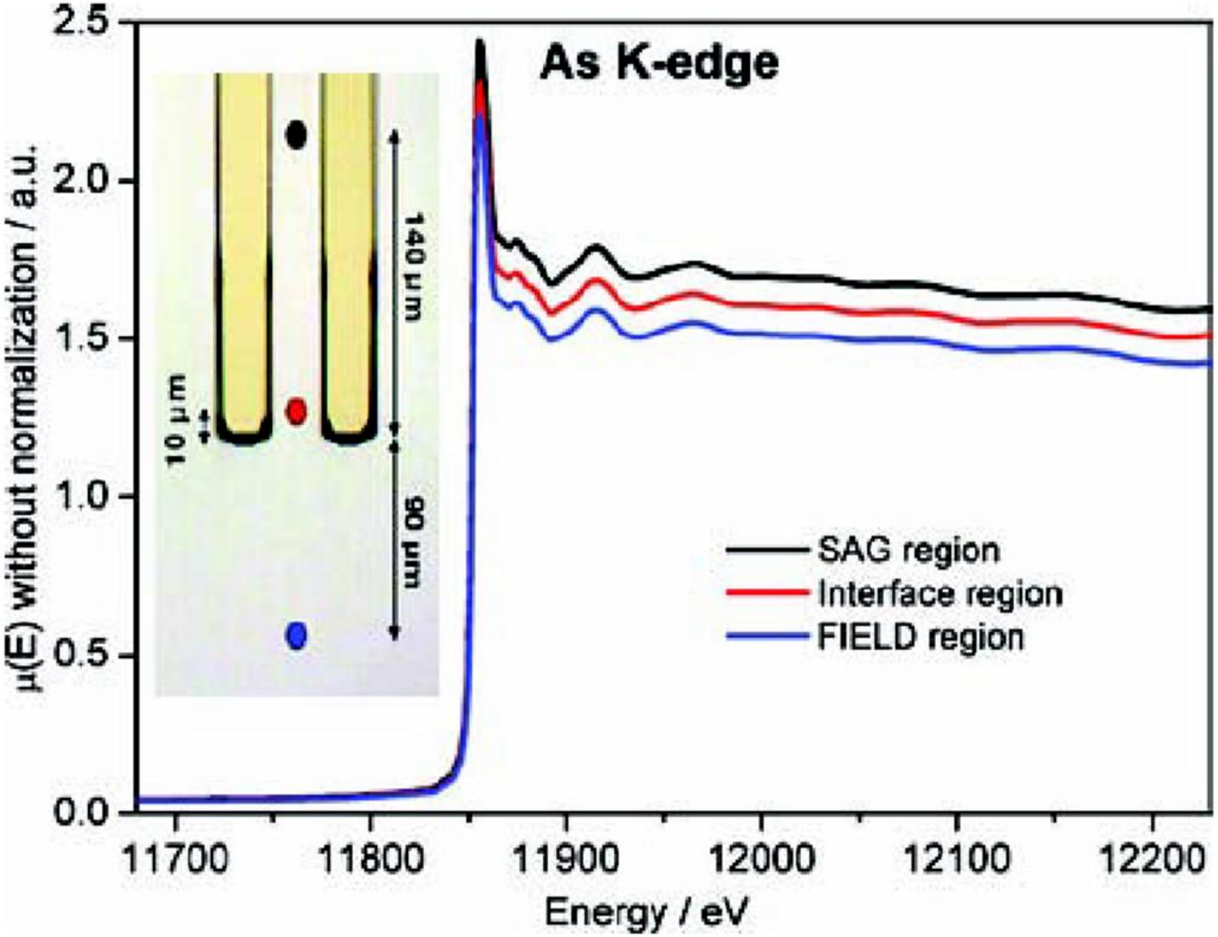

Local structural information on the $In_xGa_yAl_{1-x-y}As$ semiconductor combining micro-XAS at the Ga K-edge and As K-edge

EXAFS signal extraction

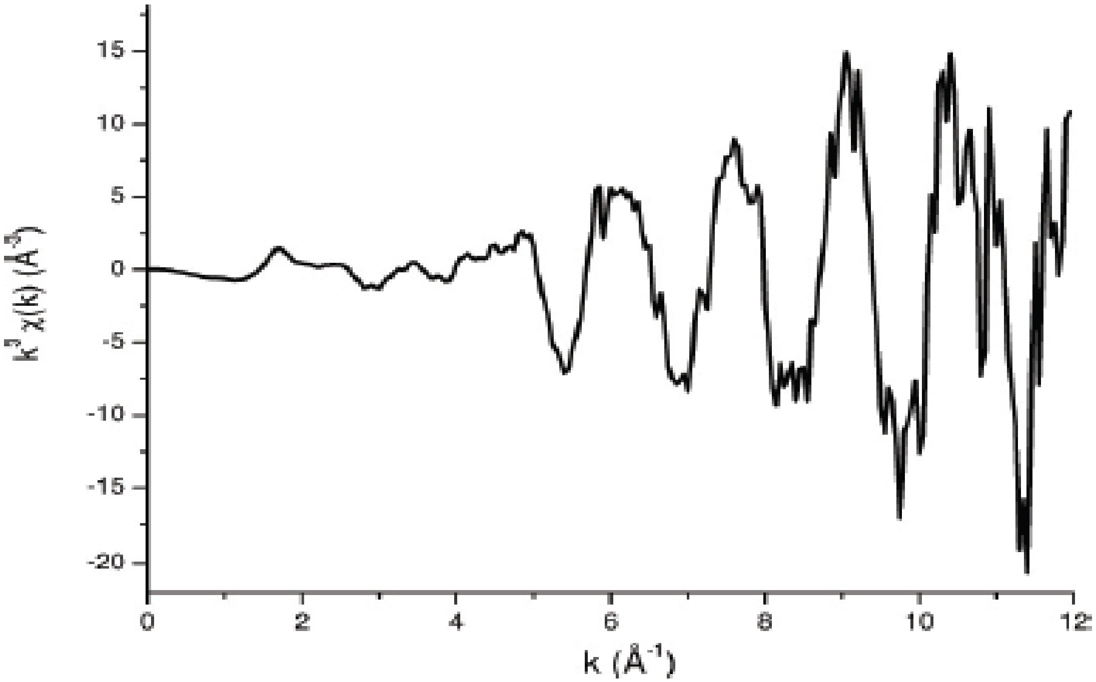

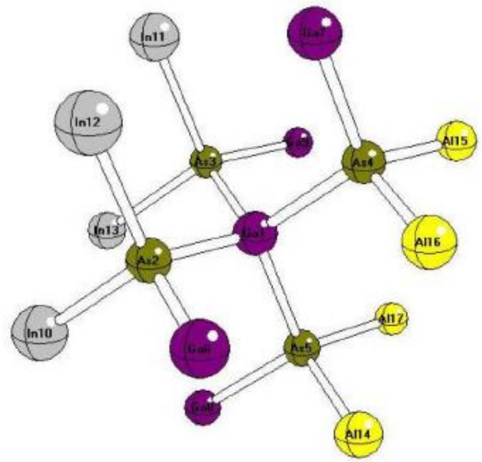

EXAFS signal:

$$\chi = \frac{\mu - \mu_0}{\mu_0}$$

$$\chi(k) = \sum_j \frac{N_j}{R_j^2} e^{-2\frac{R}{\lambda}} e^{-2k^2\sigma_j^2} A_j(k,\pi) \sin[2kR_j + \varphi(k, R_j, \pi)]$$

EXAFS data fitting

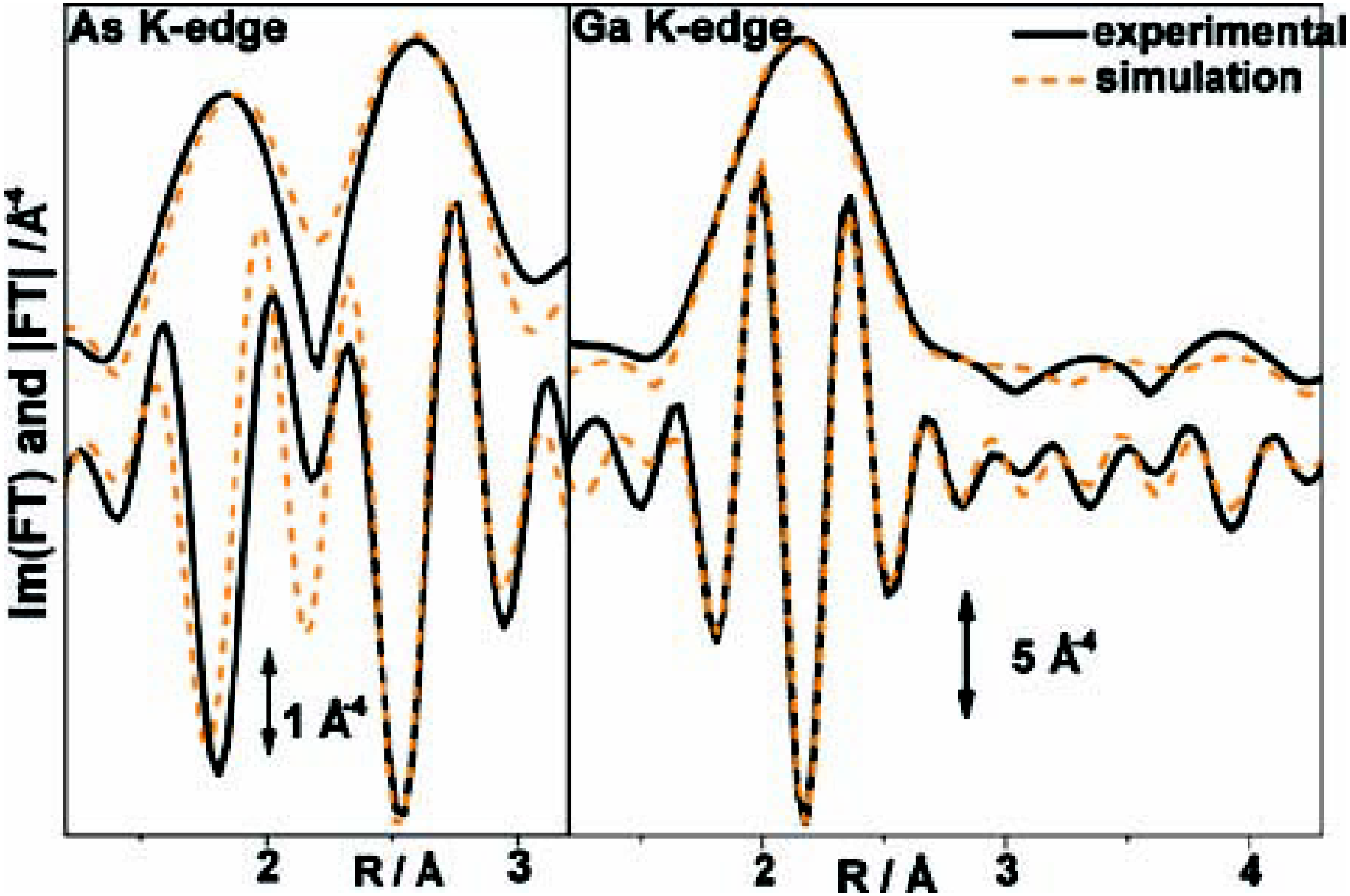

L. Mino et al., Small 2011, 7, 930-938

For the fit a co-refinement approach was adopted using the following intervals in k- and R-spaces: 3.0−9.0 $Å^{-1}$ and 1.0−3.2 Å for As K-edges, 3.0−10.8 $Å^{-1}$ and 1.0−4.3 Å for Ga K-edges

EXAFS results

Parameter	SAG	FIELD
$R_{As\text{-}Ga}$ [Å]	2.469 ± 0.007	2.463 ± 0.005
$\Delta R_{As\text{-}Ga}$ [Å]	0.021 ± 0.007	0.015 ± 0.005
$R_{As\text{-}In}$ [Å]	2.60 ± 0.02	2.60 ± 0.02
$\Delta R_{As\text{-}In}$ [Å]	-0.02 ± 0.02	-0.02 ± 0.02
$R_{As\text{-}Al}$ [Å]	2.49 ± 0.11	2.48 ± 0.11
$\sigma^2_{As\text{-}Ga}$ [Å^2]	0.006 ± 0.002	0.005 ± 0.002
$\sigma^2_{As\text{-}In}$ [Å^2]	0.008 ± 0.003	0.007 ± 0.003
$\sigma^2_{As\text{-}Al}$ [Å^2]	0.010 ± 0.004	0.008 ± 0.004

L. Mino et al., Small 2011, 7, 930-938

Further reading

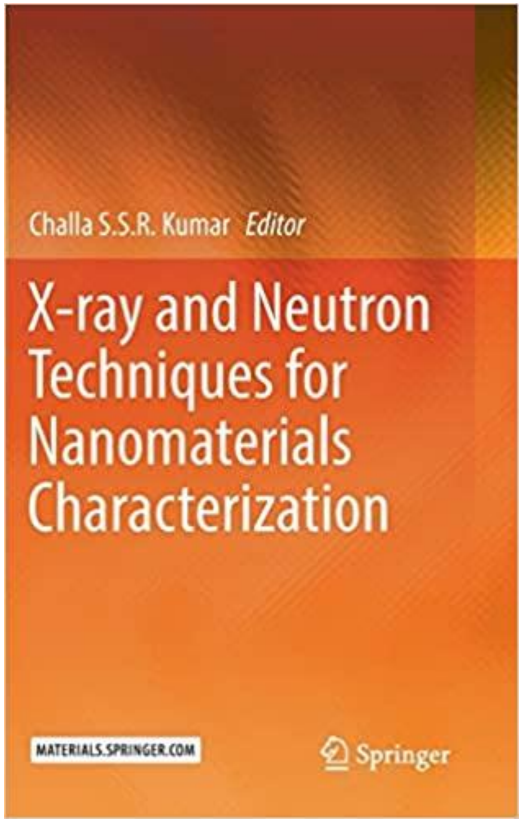

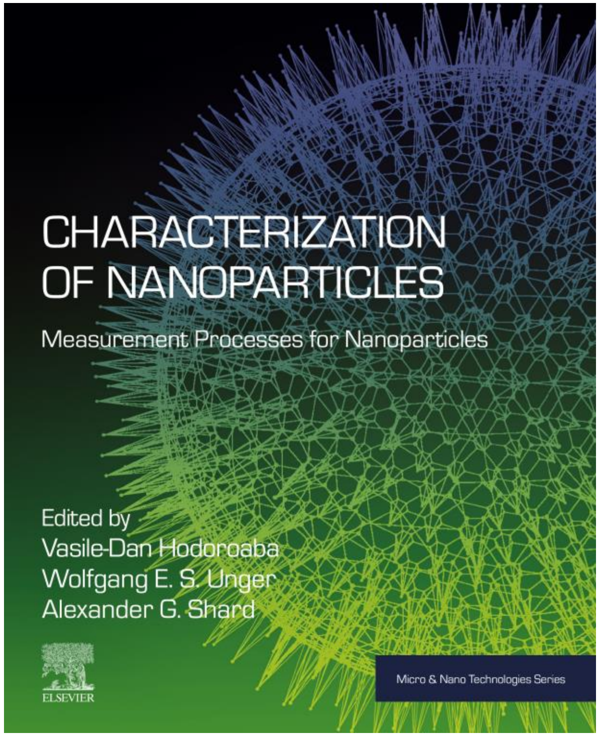

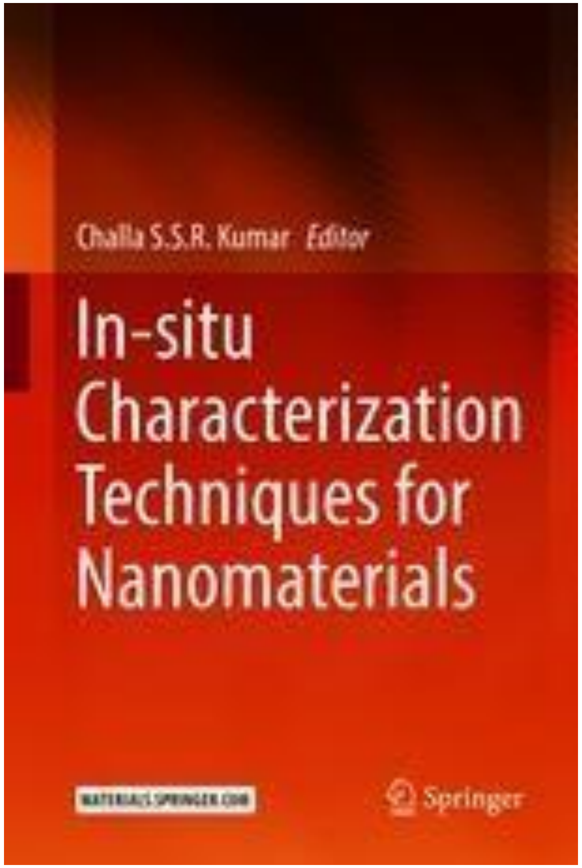

Further reading

IOP PUBLISHING JOURNAL OF PHYSICS D: APPLIED PHYSICS
J. Phys. D: Appl. Phys. **46** (2013) 423001 (72pp) doi:10.1088/0022-3727/46/42/423001

TOPICAL REVIEW

Low-dimensional systems investigated by x-ray absorption spectroscopy: a selection of 2D, 1D and 0D cases

Lorenzo Mino[1], Giovanni Agostini[1], Elisa Borfecchia[1],
Andrea Piovano[3], Erik Gallo[1,4] and Carlo Lamberti[1]

Progress in Materials Science 112 (2020) 100667

Contents lists available at ScienceDirect

Progress in Materials Science

ELSEVIER

journal homepage: www.elsevier.com/locate/pmatsci

Watching nanomaterials with X-ray eyes: Probing different length scales by combining scattering with spectroscopy

Cinzia Giannini[a], Vaclav Holy[b,c], Liberato De Caro[a], Lorenzo Mino[d], Carlo Lamberti[e,f]

Materials characterization by synchrotron x-ray microprobes and nanoprobes

Lorenzo Mino, Elisa Borfecchia, Jaime Segura-Ruiz, Cinzia Giannini, Gema Martinez-Criado, and Carlo Lamberti

Rev. Mod. Phys. **90**, 025007 – Published 28 June 2018

Thank you for your attention!